

1 Future snowfall in the Alps: Projections based on the EURO- 2 CORDEX regional climate models

3 Prisco Frei, Sven Kotlarski, Mark A. Liniger, Christoph Schär

6 - Response to Referees –

8 General

9 We thank the three referees for their careful revision of the manuscript and for their constructive comments.
10 Please find below our replies to all major comments and our suggestions on how to address these issues in a
11 revised manuscript. We hope that we satisfactorily addressed all referee comments and that the proposed
12 changes are considered as being appropriate. In case that not, we'd be looking forward to discuss individual
13 remaining issues in more detail.

14 As several referee comments addressed the RCM evaluation and the evaluation of the 2 km snowfall reference
15 itself, we'd like to put in front the following two statements on the scope of the paper:

16
17 (1) Our work is primarily concerned with the analysis of future snowfall projections. However, a basic notion on
18 the quality of raw RCM snowfall and, hence, the general ability of RCMs to represent our variable of interest is
19 required for such an exercise in our opinion. In the manuscript this is accomplished by comparing RCM raw
20 snowfall against site-scale measurements obtained from new snow sums (Figure 3). Such a comparison is
21 subject to considerable uncertainties, mostly originating from the scale gap between RCM grid cells and site-scale
22 observations and from representativity issues of observed snow cover. Due to a missing high-quality
23 observational reference at the scale of the RCM resolution (in our opinion also the HISTALP dataset has its
24 shortcomings; see below) we refrain from evaluating RCM snowfall in more detail and, at least when interpreting
25 raw snowfall change signals, implicitly assume stationary model biases. As a consequence, the projection aspect
26 of the current work is much larger than the evaluation aspect, and we tried to better clarify this issue by modifying
27 the text in Chapters 1 and 3.1. Furthermore, we adjusted the title of the manuscript accordingly and removed the
28 term "Evaluation".

29
30 (2) Relating to the previous issue but especially to the validation of the snowfall reference against which the RCM-
31 derived snowfall is adjusted: As it was already mentioned in the introduction of the original manuscript, we do not
32 claim to present an ultimate solution for bias-adjusting RCM-based snowfall but employ a spatially and temporally
33 aggregated adjustment procedure that does nevertheless separately account for temperature and precipitation
34 biases. Aspects of the snowfall climate that are not corrected for, such as details of the spatial snowfall pattern,
35 are described in Sections 2.6 and 3.3. The simplifications also include the fact that we basically accept a non-
36 perfect observation-based reference. A well-validated and appropriate reference does not exist in our opinion (see
37 also above). The very core of our work is the analysis of projected future snowfall changes and the comparison of
38 three different ways to produce such estimates: (1) Raw RCM snowfall, (2) RCM snowfall as separated from
39 simulated temperature and precipitation, and (3) RCM snowfall as separated from simulated temperature and
40 precipitation and additionally bias-adjusted. The latter version is the basic dataset for the climate scenario
41 analysis as it can be constructed for all participating RCMs (raw snowfall is not available for all of them) and as it
42 is, in principle, able to account for temperature-dependent and hence non-stationary snowfall biases. However,
43 Chapter 5.3 shows that relative change estimates largely agree among all three datasets and are robust. From
44 that point of view, the influence of remaining inaccuracies in the bias-adjusted snowfall projections due to
45 inaccuracies of the reference is presumably small. In the revised version we now try to better clarify these issues
46 by modifying Chapters 1, 2.5, 2.6 and 5.3.

47 Response to Referee #3

48 **Comment** *Half-way the introduction (lines 75-80) the authors write " Within the last few years ..." followed by "Most of these analyses are based*
49 *on GCM output or older generations of RCM ensembles at comparatively low spatial resolution : : ". This may indeed be the case for most of the*
50 *studies cited in the sentence before, but not for all of them, and the authors should specify explicitly which of them is the exception, and how that*
51 *study. compares with their work. E.g. Piazza et al. use, amongst other models, a number of RCMs operated at 12 km resolution, the study by de*
52 *Vries et al. (2014) is based on a 8-member ensemble of EC-EARTH-RACMO simulations at 12km resolution (historical and rcp8.5) configured on*
53 *a smaller domain, but in principle quite comparable to the simulations used in this paper.*

54 **Response and changes to manuscript** You are perfectly right, thanks for pointing this out. We added further
55 information on the existing RCM-based studies in this section. Furthermore, reference to the mentioned works
56 had already been given in the conclusions of the original manuscript.

57 **Comment** *Instead of using "bias correction" I would strongly recommend to use the phrase "bias adjustment" as was also the adopted terminology*
58 *by the EURO-CORDEX community. The word "correction" suggests there is a well-established methodology including a ground truth observed*

59 state which we all agree on. This is obviously not the case. It is therefore much better to use the word “adjustment” which automatically triggers
60 the questions “how” and “to what” or “in which context” as it should be.

61 **Response and changes to manuscript** We are aware of the current discussion on this issue and basically
62 agree with the referee’s suggestion. There are pros and cons to it, however. The term “bias correction” is currently
63 used and better understood by a wider community and is also better reflected by the available literature. But
64 exactly due to the points mentioned we agree that “bias adjustment” is the more suitable term. We therefore
65 changed “bias correction” (“bias-corrected”) to “bias adjustment” (“bias-adjusted”) throughout the entire
66 manuscript. This also involves modifications to the legend of Figure 13. Accordingly, we also changed “RCM_{sep+bc}”
67 (“RCM_{sep+nbc}”) to “RCM_{sep+ba}” (“RCM_{sep+nba}”). In Chapter 2.6 we include the following sentence outlining the
68 reasons behind the choice of the term: “Note that we deliberately employ the term bias adjustment as opposed to
69 bias correction to make clear that only certain aspects of the snowfall climate are adjusted and that the resulting
70 dataset might be subject to remaining inaccuracies.”

71 **Comment** In section 2.2 it is mentioned that all GCM-driven EUR-11 simulations for which control, RCP4.5 and RCP8.5 runs are currently
72 available have been included in the study. This can obviously not be a correct state of affairs. Currently means “at the moment” and since the
73 number of simulations published in the ESGF-archive is still growing, there will be a moment that the statement is no longer true. In fact, already in
74 October 2016 there were 16 simulations that met the criteria set by the authors. In addition to the their selection there were results published from
75 HadGEM2-RACMO and MPI-ESM (r2i1p1)-REMO. In April 2016, none of the two MPI-ESM-REMO simulations were available, but the HadGEM2-
76 RACMO simulation was, albeit based on version v1 which was replaced by version v2 in August 2016. So, a) you need to specify currently, and b),
77 either include the simulations that were in the archive but not in your selection, or convincingly explain why some simulations were not selected.

78 **Response and changes to manuscript** You are completely right, thanks for pointing this out. We’re now providing the
79 date on which the ESGF database was accessed for the purpose of this paper. And we also provide the reasons for not
80 including two of the available experiments. HadGEM2-RACMO was disregarded due to serious snow accumulation issues over
81 the Alps with obvious feedbacks on temperature (which is used in the snowfall separation process). MPIM-REMO realization 2
82 was disregarded as our purpose was to assess model uncertainty by employing an ensemble analysis and not internal climate
83 variability (realization 1 is contained in our ensemble, see also footnote of Table 1 in the original manuscript).

84 **Comment** Following the previous point, it is important mentioning that three different realizations of ICHEC-EC-EARTH are used to force four
85 different RCMs: r12i1p1 is used to force CCLM and RCA, r3i1p1 is used for HIRHAM, and r1i1p1 for RACMO. Different realizations of a GCM can
86 show distinct behavior owing to long-term large-scale natural variability implying that differences between the EC-EARTH forced RCM simulations
87 are not only due to differences in the RCMs. This would only hold for the CCLM and RCA simulations forced with r12i1p1. Please, mention this
88 aspect when introducing the 14 GCM-RCM chains.

89 **Response and changes to manuscript** Thanks a lot, this fact is now mentioned in the Caption of Table 1. It is,
90 however, of minor importance for the present study, as for instance the influence of the driving GCM is not
91 analyzed in detail but only mentioned at one point in the manuscript.

92 **Comment** In section 2.5 the methodology to separate snowfall from total precipitation is discussed (Richards method). In the final paragraph a
93 parametric formulation $f_{s,Ri}$ is introduced (Eqs 4-7) to express the snowfall fraction in terms of coarse-grid temperature T_k , the topographic
94 standard deviation h of the designated grid cell, and a number of constants (E,F,G,H) which are determined through an empirical fitting procedure.
95 The function $f_{s,Ri}$ is meant to be used to separate snowfall in the RCMs as well (line 282-283). Since the subgrid-scale orographic variance
96 parameter of the model orography is not known (at least this parameter is not in the ESGF-archive) I presume the authors have used h from the
97 observational dataset. Somehow the observational h and model height should match. This is not guaranteed a priori. The authors already mention
98 that orography fields from different RCMs can be quite different from each other, and from the observations (line 157-159). The authors should
99 explain how they deal with such mismatches.

100 **Response and changes to manuscript** The origin of the “observed” high resolution topography (GTOPO30) is
101 now properly referenced. This information was indeed missing so far. Concerning a potential mismatch between
102 mean grid cell topography of the RCM and mean grid cell topography as obtained from GTOPO30 we do not
103 believe that this leads to any problem. The parameterizations in the Richard method rely on topographic variance
104 at a subgrid level only, not on mean topography. We assume that this variance is properly represented by
105 GTOPO30. In any case, the relation is later on fitted again (see Figure S1). Whether the models internally work
106 with a similar topographic variance or not is not relevant here in our opinion. Nevertheless we now explicitly
107 mention this apparent and potential mismatch of mean orographies in Section 2.5.

108 **Comment** In section 2.6 the bias adjustment approach is discussed. I was surprised to see that after the detailed treatment of snowfall separation,
109 the adjustment of temperature has been dealt with so crudely. While according to Fig S4 the temperature bias considerably depends on elevation
110 the authors have chosen the shifted fractionation temperature to be independent of elevation. According to Fig 4 the adjusted fractionation
111 temperature and the temperature bias (one point per GCM-RCM realization) show considerable scatter around a linear relation, but it is not at all
112 clear and also not explained what causes this scatter. It might be due to bias depending on elevation, but also to month of the year and/or region.
113 Or is there something else? The authors should discuss their treatment of shifting the fractionation temperature in more detail, it is particularly
114 relevant because the snow fractionation temperature appears to be a crucial, and probably also a sensitive, parameter in the analysis.

115 **Response and changes to manuscript** Thanks very much for pointing out this issue. We agree that our bias
116 correction is approximate only. For instance, it only targets spatially and temporally averaged mean snowfall but
117 not the spatial pattern (see Figure 6). These limitations are actually mentioned. More sophisticated methods can
118 be thought of, but bear the danger of overparameterisation and often require a more accurate observational
119 reference. The bias adjustment of snowfall in the frame of the present paper is only one of three postprocessing
120 methods (in addition to raw = no postprocessing and separation only but no bias adjustment). See also our replies
121 in the very beginning of this document. In the end, we find that relative change signals of snowfall indices closely
122 agree no matter what the postprocessing is. Concerning the adjustment of the fractionation temperature: the bulk
123 adjustment for the entire domain is mainly based on our target (domain mean snowfall). Adjusting separately for
124 individual elevation intervals might be a better account of elevation-dependent temperature biases but would

125 probably over-interpret the uncertain snowfall reference in terms of its elevation dependency. This is mentioned
126 now in the revised version of the manuscript (Section 2.6). Regarding the relation between mean temperature
127 bias and adjusted fractionation temperature: There are several potential reasons for deviations from a linear
128 relation. In addition to the ones mentioned in your comments, also differences in daily temperature variability or in
129 the bivariate temperature-precipitation distribution can be thought of. In the revised manuscript we now mention
130 potential reasons in more detail.

131 **Comment Line 565-566:** *The sentence "Previous studies : : : with this theory (e.g. Allen and Ingram, 2002; Ban et al. 2015)" is completely out of*
132 *context. I strongly suggest to omit this sentence and the corresponding references. The focus of the Ban et al. paper is on summertime*
133 *convectively driven sub-daily (hourly) precipitation extremes and its relation with temperature. This is miles away from the Sq99 and S1d snowfall*
134 *parameters used in this paper to indicate heavy (but not extreme) snowfall at the daily scale outside the summer season.*

135 **Response and changes to manuscript** It is certainly true that we neither deal with sub-daily extremes nor with
136 the very tail of the daily snowfall distribution. However, we still believe that this information is relevant and not out
137 of context as it presents general evidence for applicability of the C-C-relation concerning precipitation extremes.
138 We'd therefore like to refrain from removing this sentence, but tried to better clarify the fact that different variables
139 are addressed in the cited works.

140 **Further minor comments**

141 **Response and changes to manuscript** Thank you very much for these additional comments and ideas! All
142 suggested further minor corrections were implemented with the exception of comment 28 (Sorry, this one is not
143 clear to us) and comment 29 (If left up to us, we'd prefer to stick to the current color scheme which is intuitive in
144 our opinion and still allows to grasp the important characteristics of the spatial distribution).

145 **Further changes to the manuscript**

146 **Chapter 2.1 "Observational data"** For reasons of completeness we additionally included the information that the
147 temperature and precipitation grids employed are slightly shifted with respect to their reference time interval
148 (midnight UTC - midnight UTC for temperature, 06 UTC - 06 UTC for precipitation).

149 **Chapter 2.2 "Climate model data"** In the last paragraph we erroneously spoke of *six* RCMs considered. We
150 corrected this to *seven* RCMs.

151 **Chapter 3.1** To better account for uncertainties in this simplified evaluation we now additionally cite the work of
152 Grünewald and Lehning (2015) that highlights the danger of non-representativity of single-site snow depth
153 observations in Alpine terrain.

154 **Figure 3** In the left panel two of the 29 stations employed (WFJ and MVE) were plotted at a wrong elevation in
155 the original version. For both stations the correct elevation differs by about 100 m from the previously used
156 elevation. The figure has been corrected accordingly, in addition to the modifications to this figure mentioned
157 above. The conclusions of the analysis do not change.

158 **Overall manuscript** Several minor spelling and wording mistakes as well as an inconsistent use of past and
159 present tense were corrected.

160

161

162

Future sSnowfall in the Alps: ~~Evaluation~~ and pProjections based on the EURO-CORDEX regional climate models

Prisco Frei¹, Sven Kotlarski^{2,*}, Mark A. Liniger², Christoph Schär¹

¹ Institute for Atmospheric and Climate Sciences, ETH Zurich, [CH-8006](#), Zurich, Switzerland

² Federal Office of Meteorology and Climatology, MeteoSwiss, [CH-8058](#) Zurich-Airport, Switzerland

* Corresponding author: sven.kotlarski@meteoswiss.ch

Abstract. Twenty-first century snowfall changes over the European Alps are assessed based on high-resolution regional climate model (RCM) data made available through the EURO-CORDEX initiative. Fourteen different combinations of global and regional climate models with a target resolution of 12 km, and two different emission scenarios are considered. As raw snowfall amounts are not provided by all RCMs, a newly developed method to separate snowfall from total precipitation based on near-surface temperature conditions and accounting for subgrid-scale topographic variability is employed. The evaluation of the simulated snowfall amounts against an observation-based reference indicates the ability of RCMs to capture the main characteristics of the snowfall seasonal cycle and its elevation dependency, but also reveals considerable positive biases especially at high elevations. These biases can partly be removed by the application of a dedicated RCM bias correction-adjustment that separately considers temperature and precipitation biases.

Snowfall projections reveal a robust signal of decreasing snowfall amounts over most parts of the Alps for both emission scenarios. Domain and multi-model-mean decreases of mean September-May snowfall by the end of the century amount to -25% and -45% for RCP4.5 and RCP8.5, respectively. Snowfall in low-lying areas in the Alpine forelands could be reduced by more than -80%. These decreases are driven by the projected warming and are strongly connected to an important decrease of snowfall frequency and snowfall fraction and are also apparent for heavy snowfall events. In contrast, high-elevation regions could experience slight snowfall increases in mid-winter for both emission scenarios despite the general decrease of the snowfall fraction. These increases in mean and heavy snowfall can be explained by a general increase of winter precipitation and by the fact that, with increasing temperatures, climatologically cold areas are shifted into a temperature interval which favours higher snowfall intensities. In general, percentage changes of snowfall indices are robust with respect to the RCM postprocessing strategy employed: Similar results are obtained for raw, separated and separated + bias-adjusted snowfall amounts. Absolute changes, however, can differ among these three methods.

201 1 Introduction

202 Snow is an important resource for the Alpine regions, be it for tourism, hydropower generation, or
203 water management (Abegg et al., 2007). According to the Swiss Federal Office of Energy (SFOE)
204 hydropower generation accounts for approximately 55% of the Swiss electricity production (SFOE,
205 2014). Consideration of changes in snow climatology needs to address aspects of both snow cover
206 and snow-fall. In the recent past, an important decrease of the mean snow cover depth and duration in
207 the Alps was observed (e.g, Laternser and Schneebeli, 2003; Marty, 2008; Scherrer et al., 2004).
208 ~~Future p~~Projections of future snow cover changes based on using climate model simulations ~~of the~~
209 ~~anthropogenic greenhouse effect~~ indicate a further substantial reduction (Schmucki et al., 2015a;
210 Steger et al., 2013), strongly linked to the expected rise of temperatures (e.g., CH2011, 2011; Gobiet
211 et al., 2014). On regional and local scales rising temperatures exert a direct influence on snow cover in
212 two ways: First, total snowfall sums are expected to decrease by a ~~decreasing-lower~~ probability for
213 precipitation to fall as snow implying and a decreasing snowfall fraction (ratio between solid and total
214 precipitation). Second, snow on the ground is subject to faster and accelerated melt. These warming-
215 induced trends might be modulated by changes in atmospheric circulation statistics~~patterns~~.

216 Although the snowfall fraction is expected to decrease ~~at lower elevations~~ during the 21st century
217 (e.g., Räisänen, 2016), extraordinary snowfall events can still leave a trail of destruction. A recent
218 example was the winter 2013/2014 with record-breaking heavy snowfall events along the southern rim
219 of the European Alps (e.g., Techel et al., 2015). The catastrophic effects of heavy snowfall range from
220 avalanches and floods to road or rail damage. In extreme cases these events can even result in the
221 weight-driven collapse of buildings or loss of human life (Marty and Blanchet, 2011). Also mean
222 snowfall conditions, such as the mean number of snowfall days in a given period, can be of high
223 relevance for road management (e.g. Zubler et al., 2015) or airport operation. Projections of future
224 changes in ~~the snowfall-climate~~, including mean and extreme conditions, are therefore highly relevant
225 for long-term planning and adaptation purposes in order to assess and prevent related socio-economic
226 impacts and costs.

227 21st century climate projections typically rely on climate models. For large-scale projections, global
228 climate models (GCMs) with a rather coarse spatial resolution of 100 km or more are used. ~~For~~
229 assessing~~To assess~~ regional to local scale impacts, where typically a much higher spatial resolution
230 ~~of the projections~~ is required, a GCM can be dynamically downscaled by nesting a regional climate
231 model (RCM) over the specific domain of interest (Giorgi, 1990). In such a setup, the GCM provides
232 the lateral and sea surface boundary conditions to the RCM. One advantage of climate models is the
233 ability to estimate climate change in a physically based manner under different greenhouse gas (GHG)
234 emission scenarios. With the Intergovernmental Panel on Climate Change's (IPCC) release of the Fifth
235 Assessment Report (AR5; IPCC, 2013) the so-called representative concentration pathway (RCP)
236 scenarios have been introduced (Moss et al., 2010) which specify GHG concentrations and
237 corresponding emission pathways for several radiative forcing targets. To estimate inherent projection
238 uncertainties, ensemble approaches employing different climate models, different greenhouse gas
239 scenarios, and/or different initial conditions are being used (e.g., Deser et al., 2012; Hawkins and
240 Sutton, 2009; Rummukainen, 2010).

241 Within the last few years several studies targeting the future global and European snowfall evolution
242 based on climate model ensembles were carried out (e.g., de Vries et al., 2013; de Vries et al., 2014;
243 Krasting et al., 2013; O’Gorman, 2014; Piazza et al., 2014; Räisänen, 2016; Soncini and Bocchiola,
244 2011). Most of these analyses are based on GCM output or older generations of RCM ensembles at
245 comparatively low spatial resolution, which are not able to properly resolve snowfall events over
246 regions with complex topography. New generations of high resolution RCMs are a first step toward an
247 improvement on this issue. This is in particular true for the most recent high-resolution regional climate
248 change scenarios produced by the global CORDEX initiative (Giorgi et al., 2009) and its European
249 branch EURO-CORDEX (Jacob et al., 2014). The present work aims to exploit this recently
250 established RCM archive with respect to future snowfall conditions over the area of the European
251 Alps. It thereby complements the existing works of Piazza et al. (2014) and de Vries et al. (2014) who
252 among others also exploit comparatively high-resolved RCM experiments (partly originating from
253 EURO-CORDEX as well) but with a reduced ensemble size and/or not specifically targeting the entire
254 Alpine region.

255 In general and on decadal to centennial time scales, two main drivers of future snowfall changes over
256 the European Alps with competing effects on snowfall amounts are apparent from the available
257 literature: (1) Mean winter precipitation is expected to increase over most parts of the European Alps
258 and in most EURO-CORDEX experiments (e.g., Rajczak et al., in prep.; Smiatek et al., 2016) which in
259 principle could lead to higher snowfall amounts. (2) Temperatures are projected to considerably rise
260 throughout the annual cycle (e.g., Gobiet et al., 2014; Smiatek et al., 2016; Steger et al., 2013) with
261 the general effect of a decreasing snowfall frequency and fraction, thus potentially leading to a
262 reduction in overall snowfall amounts. Separating the above two competing factors is one of the
263 targets of the current study. A potential complication is that changes in daily precipitation frequency
264 (here events with precipitation > 1 mm/day) and precipitation intensity (average amount on wet days)
265 can change in a counteracting manner (e.g., Fischer et al., 2015; Rajczak et al., 2013), and that
266 relative changes are not uniform across the event category (e.g. Ban et al., 2015; Fischer and Knutti,
267 2016).

268 We here try to shed more light on these issues by addressing the ~~By covering both model evaluation~~
269 ~~and high-resolution future snowfall projections we are addressing the~~ following main objectives:

270 **Snowfall separation on an ~~(coarse resolution)~~ RCM grid.** Raw snowfall outputs are not available
271 for all members of the EURO-CORDEX RCM ensemble ~~and, furthermore, a gridded observational~~
272 ~~snowfall product that could serve as reference for RCM evaluation does not exist.~~ Therefore, an
273 adequate snowfall separation technique, i.e., the derivation of snowfall amounts based on readily
274 available daily near-surface air temperature and precipitation data, is required. Furthermore, ~~as the~~
275 ~~observational and simulated grids of the two latter variables are typically not available at the same~~
276 ~~horizontal resolution,~~ we seek for a snowfall separation method that accounts for the topographic
277 subgrid-scale variability of snowfall on ~~the the coarser (RCM)~~ grid.

278 **Snowfall bias ~~correction~~ adjustment.** Even the latest generation of RCMs is known to suffer from
279 systematic model biases (e.g., Kotlarski et al., 2014). In GCM-driven setups as employed within the

280 present work these might partly be inherited from the driving GCM. To remove such systematic model
281 biases in temperature and precipitation, a simple bias ~~correction-adjustment~~ methodology ~~is~~ will be
282 developed and employed in the present work. To assess its performance and applicability, different
283 snowfall indices in the bias-~~corrected-adjusted~~ and not bias-~~corrected-adjusted~~ output are ~~will be~~
284 compared against observation-~~based~~ estimates.

285 **Snowfall projections for the late 21st century.** Climate change signals for various snowfall indices
286 over the Alpine domain and for specific elevation intervals, derived by a comparison of 30-year control
287 and scenario periods, are ~~will be~~ analysed under the assumption of the RCP8.5 emission scenario. In
288 addition, we aim to identify and quantify the main drivers of future snowfall changes and, in order to
289 assess emission scenario uncertainties, compare RCP8.5-based results with experiments assuming
290 the more moderate RCP4.5 emission scenario. Snowfall projections are generally based on three
291 different datasets: (1) raw RCM snowfall where available, (2) RCM snowfall separated from simulated
292 temperature and precipitation, and (3) RCM snowfall separated from simulated temperature and
293 precipitation and additionally bias-adjusted. While all three estimates are compared for the basic
294 snowfall indices in order to assess the robustness of the projections, more detailed analyses are
295 based on dataset (3) only.

296 In addition and as preparatory analysis, we carry out a basic evaluation of RCM-simulated snowfall
297 amounts. This evaluation, however, is subject to considerable uncertainties as a high-quality
298 observation-based reference at the required spatial scale is not available, and the very focus of the
299 present work is laid on the snowfall projection aspect.

300 ~~On centennial time scales, two main drivers of future snowfall changes over the European Alps with~~
301 ~~competing effects on snowfall amounts are apparent: (1) Mean winter precipitation is expected to~~
302 ~~increase over most parts of the European Alps and in most EURO-CORDEX experiments (e.g.,~~
303 ~~Rajczak et al., in prep.; Smiatek et al., 2016) which in principle could lead to higher snowfall amounts.~~
304 ~~(2) Temperatures are projected to considerably rise throughout the annual cycle (e.g., Gobiet et al.,~~
305 ~~2014; Smiatek et al., 2016; Steger et al., 2013) with the general effect of a decreasing snowfall~~
306 ~~frequency and fraction, thus potentially leading to a reduction in overall snowfall amounts changes.~~
307 ~~Separating the above two competing factors is one of the targets of the current study. A potential~~
308 ~~complication is that changes in daily precipitation frequency (here events > 1 mm/day) and~~
309 ~~precipitation intensity (average amount on wet days) can change in a counteracting manner (e.g.,~~
310 ~~Fischer et al., 2015; Rajczak et al., 2013), and that relative changes are not uniform across the event~~
311 ~~category (e.g. Ban et al., 2015; Fischer and Knutti, 2016).~~

312 The article is structured as follows: Section 2 describes the data used and methods employed. In
313 Sections 3 and 4 results of the bias ~~correction-adjustment~~ approach and snowfall projections for the
314 late 21st century are shown, respectively. The latter are further discussed in Section 5 while overall
315 conclusions and a brief outlook are provided in Section 6. Additional supporting figures are provided in
316 the supplementary material (prefix 'S' in Figure numbers).

317 2 Data and methods

318 2.1 Observational data

319 To estimate observation-based snowfall, two gridded data sets, one for precipitation and one for
320 temperature, derived from station observations and covering the area of Switzerland are used. Both
321 data sets are available on a daily basis with a horizontal resolution of 2 km for the entire evaluation
322 period 1971-2005 (see Sec. 2.3).

323 The gridded precipitation data set (RhiresD) represents a daily analysis based on a high-resolution
324 rain-gauge network (MeteoSwiss, 2013a) consisting of more than 400 stations which has that have a
325 balanced distribution in the horizontal but under-represents high altitudes (Frei and Schär, 1998; Isotta
326 et al., 2014; Konzelmann et al., 2007). Albeit the data set's resolution of 2 km, the effective grid
327 resolution as represented by the mean inter-station distance is about 15 - 20 km and thus comparable
328 to the nominal resolution of the available climate model data (see Sec. 2.2). The dataset has not been
329 corrected for the systematic measurement bias of rain gauges (e.g., Neff, 1977; Sevruk, 1985; Yang et
330 al., 1999).

331 The gridded near-surface air temperature (from now on simply referred to as *temperature*) data set
332 (TabsD) utilises a set of approx. 90 homogeneous long-term station series (MeteoSwiss, 2013b).
333 Despite the high quality of the underlying station series, errors might be introduced by unresolved
334 scales, an uneven spatial distribution and interpolation uncertainty (Frei, 2014). The unresolved effects
335 of land cover or local topography, for instance, probably lead to an underestimation of spatial
336 variability. ~~Another problem arises in inner Alpine valleys, where the presence of cold air pools is~~
337 ~~systematically overestimated. Also note that, while RhiresD provides daily precipitation sums~~
338 ~~aggregated from 6 UTC to 6 UTC of the following day, TabsD is a true daily temperature average from~~
339 ~~midnight UTC to midnight UTC. Due to a high temporal autocorrelation of daily mean temperature this~~
340 ~~slight inconsistency in the reference interval of the daily temperature and precipitation grids is~~
341 ~~expected to not systematically influence our analysis.~~

342 In addition to the gridded temperature and precipitation datasets and in order to validate simulated raw
343 snowfall amounts station-based observations of fresh snow sums (snow depth) at daily resolution from
344 29 stations in Switzerland with data available for at least 80% of the evaluation period 1971-2005 are
345 employed.

346 2.2 Climate model data

347 In terms of climate model data we exploit a recent ensemble of regional climate projections made
348 available by EURO-CORDEX (www.euro-cordex.net), the European branch of the World Climate
349 Research Programme's CORDEX initiative (www.cordex.org; Giorgi et al., 2009). RCM simulations for
350 the European domain were run at a resolution of approximately 50 km (EUR-44) and 12.5 km (EUR-
351 11) with both re-analysis boundary forcing (Kotlarski et al., 2014; Vautard et al., 2013) and GCM-
352 forcing (Jacob et al., 2014). ~~We here disregard the reanalysis-driven experiments and employ the. The~~
353 ~~latter include GCM-driven simulations only. These include~~ historical control simulations and future
354 projections based on RCP greenhouse gas and aerosol emission scenarios. Within the present work

355 we employ daily averaged model output of all except two¹GCM-driven EUR-11 simulations for which
356 control, RCP4.5 and RCP8.5 runs are currently were available in December 2016. This yields a total
357 set of 14 GCM-RCM model chains, combining five driving GCMs with seven different RCMs (Tab. 1).
358 We exclusively focus on the higher resolved EUR-11 simulations and disregard the coarser EUR-44
359 ensemble due to the apparent added value of the EUR-11 ensemble with respect to regional-scale
360 climate features in the complex topographic setting of the European Alps (e.g., Giorgi et al., 2016;
361 Torma et al., 2015).

362 It is important to note that each of the sevensix RCMs considered uses an individual grid cell
363 topography field. Model topographies for a given grid cell might therefore considerably differ from each
364 other, and also from the observation-based orography. Hence, it is not meaningful to compare snowfall
365 values at individual grid cells since the latter might be situated at different elevations. Therefore, most
366 analyses of the present work were carried out as a function of elevation, i.e., by averaging climatic
367 features over distinct elevation intervals.

368 **2.3 Analysis domain and periods**

369 The arc-shaped European Alps - with a West-East extent of roughly 1200 km , a total of area 190'000
370 km² and a peak elevation of 4810 m a.s.l. (Mont Blanc) - are the highest and most prominent
371 mountain range which is entirely situated in Europe. In the present work, two different analysis
372 domains are used. The evaluation of the bias correction-adjustment approach depends on the
373 observational data sets RhiresD and TabsD (see Sec. 2.1). As these cover Switzerland only, the
374 evaluation part of the study (Sec. 3) is constrained to the Swiss domain (Fig. 1, bold line). For the
375 analysis of projected changes of different snowfall indices (Sec. 4 and 5) a larger domain covering the
376 entire Alpine crest with its forelands is considered (Fig. 1, coloured region).

377 Our analysis is based on three different time intervals. The evaluation period (EVAL) 1971-2005 iswas
378 used for the calibration and validation of the bias correction-adjustment approach. Future changes of
379 snowfall indices are were computed by comparing a present-day control period (1981-2010, CTRL) to
380 a future scenario period at the end of the 21st century (2070-2099, SCEN). For all periods (EVAL,
381 CTRL and SCEN), the summer months June, July and August (JJA) are excluded from any statistical
382 analysis. In addition to seasonal mean snowfall conditions, i.e., averages over the nine-month period
383 from September to May, we also analyse the seasonal cycle of individual snowfall indices at monthly
384 resolution.

385 **2.4 Analysed snowfall indices and change signals**

386 A set of six different snowfall indices is considered (Tab. 2). Mean snowfall (S_{mean}) refers to the
387 (spatio-) temporally-averaged snowfall amount in mm SWE (note that from this point on we will use the
388 term "mm" as a synonym for "mm SWE" as unit of several snowfall indices). The two indices heavy
389 snowfall (S_{q99}) and maximum 1-day snowfall ($S_{1\text{d}}$) allow the assessment of projected changes in heavy

¹ The HadGEM2-RACMO experiments were excluded due to serious snow accumulation issues over the European Alps. Furthermore, only realization 1 of MPI-M-REMO was included in order to avoid mixing GCM-RCM sampling with pure internal climate variability sampling.

390 snowfall events and amounts. S_{1d} is derived by averaging maximum 1-day snowfall amounts over all
 391 individual months/seasons of a given time period (i.e., by averaging 30 maximum values in the case of
 392 the CTRL and SCEN period), while S_{q99} is calculated from the grid point-based 99th all-day snowfall
 393 percentile of the daily probability density function (PDF) for the entire time period considered. We use
 394 all-day percentiles as the use of wet-day percentiles leads to conditional statements that are often
 395 misleading (see the analysis in Schär et al. 2016). Note that the underlying number of days differs for
 396 seasonal (September-May) and monthly analyses. Snowfall frequency (S_{freq}) and mean snowfall
 397 intensity (S_{int}) are based on a wet-day threshold of 1 mm/day and provide additional information about
 398 the distribution and magnitude of snowfall events, while the snowfall fraction (S_{frac}) describes the ratio
 399 of solid precipitation to total precipitation. As climate models tend to suffer from too high occurrence of
 400 drizzle and as small precipitation amounts are difficult to measure, daily precipitation values smaller or
 401 equal to 0.1 mm were ~~initially~~ set to zero in both the observations and the simulations prior to the
 402 remaining analyses.

403 Projections are assessed by calculating two different types of changes between the CTRL and the
 404 SCEN period. The absolute change signal (Δ) of a particular snowfall index X (see Tab.2)

$$405 \quad \Delta X = X_{SCEN} - X_{CTRL} \quad (1)$$

406 and the relative change signal (δ) which describes the change of the snowfall index as a percentage of
 407 its CTRL period value

$$408 \quad \delta X = \left(\frac{X_{SCEN}}{X_{CTRL}} - 1 \right) \cdot 100 \quad (2)$$

409 To prevent erroneous data interpretation due to possibly ~~ye~~ large relative changes of small CTRL
 410 values, certain grid boxes were masked out before calculating and averaging the signal of change.
 411 This filtering was done by setting threshold values for individual indices and statistics (see Table 2).

412 2.5 Separating snowfall from total precipitation

413 Due to (a) the lack of a gridded observational snowfall data set and (b) the fact that not all RCM
 414 simulations available through EURO-CORDEX provide raw snowfall as an output variable, a method
 415 to separate solid from total precipitation depending on near-surface temperature conditions is
 416 developed. ~~This method also allows for a more physically-based bias correction of simulated snowfall~~
 417 ~~amounts (see Sec. 2.6). Due to the temperature dependency of snowfall occurrence, snowfall biases~~
 418 ~~of a given climate model cannot be expected to remain constant under current and future (i.e.,~~
 419 ~~warmer) climate conditions. For instance, a climate model with a given temperature bias might pass~~
 420 ~~the snow-rain temperature threshold earlier or later than reality during the general warming process.~~
 421 ~~Hence, traditional bias correction approaches based only on a comparison of observed and simulated~~
 422 ~~snowfall amounts in the historical climate would possibly fail due to a non-stationary bias structure.~~

423 The simplest approach to separate snowfall from total precipitation is to fractionate the two phases
 424 binary by applying a constant snow fractionation temperature (e.g., de Vries et al., 2014; Schmucki et
 425 al., 2015a; Zubler et al., 2014). More sophisticated methods estimate the snow fraction f_s dependence

426 on air temperature with linear or logistic relations (e.g., Kienzle, 2008; McAfee et al., 2014). In our
 427 case, the different horizontal resolutions of the observational (high resolution of 2 km) and simulated
 428 (coarser resolution of 12 km) data sets further complicate a proper comparison of the respective
 429 snowfall amounts. Thus, we explicitly analysed the snowfall amount dependency on the grid resolution
 430 and exploited possibilities for including subgrid-scale variability in snowfall separation ~~based on coarse~~
 431 ~~grid information~~. This approach is important as especially in Alpine terrain a strong subgrid-scale
 432 variability of near-surface temperatures due to orographic variability has to be expected, with
 433 corresponding effects on the subgrid-scale snowfall fraction.

434 For this preparatory analysis, which is entirely based on observational data, a reference snowfall is
 435 derived. It is based on the approximation of snowfall by application of a fixed temperature threshold to
 436 daily total precipitation amounts on the high resolution observational grid (2 km) and will be termed
 437 *Subgrid method* thereafter: First, the daily snowfall S' at each grid point of the observational data set at
 438 high resolution (2 km) is derived by applying a snow fractionation temperature $T^*=2^\circ\text{C}$. The whole
 439 daily precipitation amount P' is accounted for as snow S' (i.e., $f_s=100\%$) for days with daily mean
 440 temperature $T \leq T^*$. For days with $T > T^*$, S' is set to zero and P' is attributed as rain (i.e., $f_s=0\%$). This
 441 threshold approach with a fractionation temperature of 2°C corresponds to the one applied in previous
 442 works and results appear to be in good agreement with station-based snowfall measurements (e.g.,
 443 Zubler et al., 2014). The coarse grid (12 km) reference snowfall S_{SG} is determined by averaging the
 444 sum of separated daily high resolution S' over all n high-resolution grid points i located within a specific
 445 coarse grid point k . I.e., at each coarse grid point k

$$446 \quad S_{SG} = \frac{1}{n} \cdot \sum_{i=1}^n P'_i [T'_i \leq T^*] = \frac{1}{n} \sum_{i=1}^n S'_i \quad (3)$$

447 For comparison, the same binary fractionation method with a temperature threshold of $T^*=2^\circ\text{C}$ is
 448 directly applied on the coarse 12 km grid (*Binary method*). For this purpose, total precipitation P' and
 449 daily mean temperature T' of the high-resolution data are conservatively remapped to the coarse grid
 450 leading to P and T , respectively. Compared to the *Subgrid method*, the *Binary method* neglects any
 451 subgrid-scale variability of the snowfall fraction. As a result, the *Binary method* underestimates S_{mean}
 452 and overestimates S_{q99} for ~~most~~ elevation intervals (Fig. 2). The underestimation of S_{mean} can be
 453 explained by the fact that even for a coarse grid temperature above T^* individual high-elevation
 454 subgrid cells (at which $T \leq T^*$) can receive substantial snowfall amounts, ~~a process that is not~~
 455 ~~accounted for by the Binary method~~. As positive precipitation-elevation gradients can be assumed for
 456 most parts of the domain (larger total precipitation at high elevations; see e.g. Kotlarski et al., 2012
 457 and Kotlarski et al., 2015 for an Alpine-scale assessment) the neglect of subgrid-scale snowfall
 458 variation in the Binary method hence leads a systematic underestimation of mean snowfall compared
 459 to the Subgrid method. Furthermore, following O'Gorman (2014), heavy snowfall events are expected
 460 to occur in a narrow temperature range below the rain-snow transition. As the *Binary method* in these
 461 temperature ranges always leads to a snowfall fraction of 100%, too large S_{q99} values would result.

462 To take into account these subgrid-scale effects, a more sophisticated approach – referred to as the
 463 *Richards method* – is developed here. This method is based upon a generalised logistic regression
 464 (Richards, 1959). Here, we apply this regression to relate the surface temperature T to the snow

465 fraction f_s by accounting for the topographic subgrid-scale variability. At each coarse grid-point k , the
 466 *Richards method*-based snowfall fraction $f_{s,RI}$ for a given day is hence computed as follows:

$$467 \quad f_{s,RI}(T_k) = \frac{1}{[1 + C_k \cdot e^{D_k \cdot (T_k - T^*)}]^{C_k}} \quad (4)$$

468 with C as the point of inflexion (denoting the point with largest slope), and D the growth rate D
 469 (reflecting the mean slope). T_k is the daily mean temperature of the corresponding coarse grid box k
 470 and $T^*=2^\circ\text{C}$ the snow fractionation temperature. First, we estimate the two parameters C and D of
 471 Equation 4 for each single coarse grid point k by minimizing the least-square distance to the f_s values
 472 derived by the *Subgrid method* via the reference snowfall S_{SG} (local fit). Second, C and D are
 473 expressed as a function of the topographic standard deviation σ_h of the corresponding coarse
 474 resolution grid point only (Fig. S1; global fit). This makes it possible to define empirical functions for
 475 both C and D that can be used for all grid points k in the Alpine domain and that depend on σ_h only.

$$476 \quad \sigma_{h,k} = \sqrt{\frac{\sum_i^n (h_i - \bar{h}_k)^2}{n-1}} \quad (5)$$

$$477 \quad C_k = \frac{1}{(E - \sigma_{h,k} \cdot F)} \quad (6)$$

$$478 \quad D_k = G \cdot \sigma_{h,k}^{-H} \quad (7)$$

479 Through a minimisation of the least square differences the constant parameters in Equations 6 and 7
 480 are calibrated over the domain of Switzerland and using daily data from the period September to May
 481 1971-2005 leading to values of $E=1.148336$, $F=0.000966 \text{ m}^{-1}$, $G=143.84113 \text{ }^\circ\text{C}^{-1}$ and $H=0.8769335$.
 482 Note that σ_h is sensitive to the resolution of the two grids to be compared (cf. Eq. 5). It is a measure for
 483 the uniformity of the underlying topography and has been computed based on the high-resolution
 484 [GTOPO30 digital elevation model \(https://lta.cr.usgs.gov/GTOPO30\)](https://lta.cr.usgs.gov/GTOPO30) aggregated to a regular grid of
 485 [1.25 arc seconds \(about 2 km\) which reflects the spatial resolution of the observed temperature and](#)
 486 [precipitation grids \(cf. Section 2.1\)](#). Small values of σ_h indicate a low subgrid-scale topographic
 487 variability, such as in the Swiss low-lands, while high values result from non-uniform elevation
 488 distributions, such as in areas of inner Alpine valleys. σ_h as derived from GTOPO30 might be different
 489 from the subgrid-scale topographic variance employed by the climate models themselves, which is
 490 however not relevant here as only grid cell-averaged model output is analysed and as we considere σ_h
 491 as a proper estimate of subgrid-scale variability.

492 Figure S1 (panel c) provides an example of the relation between daily mean temperature and daily
 493 snow fraction f_s for grid cells with topographical standard deviations of 50 m and 500 m, respectively.
 494 The snowfall amount S_{RI} for a particular day and a particular coarse grid box is finally obtained by
 495 multiplying the corresponding $f_{s,RI}$ and P values. A comparison with the *Subgrid method* yields very
 496 similar results. For both indices S_{mean} and S_{q99} , mean ratios across all elevation intervals are close to 1
 497 (Fig. 2). At single grid points, maximum deviations are not larger than 1 ± 0.1 . Note that for this
 498 comparison calibration and validation period are identical (EVAL period). Based on this analysis, it has
 499 been decided to separate snowfall according to the *Richards method* throughout this work in both the

500 observations and in the RCMs. The observation-based snowfall estimate obtained by applying the
501 *Richards method* to the observational temperature and precipitation grids after spatial aggregation to
502 the 0.11° RCM resolution will serve as reference for the RCM bias ~~correction~~adjustment and will be
503 termed *reference* hereafter. One needs to bear in mind that the parameters *C* and *D* of the Richards
504 method were fitted for the Swiss domain only and were later on applied to the entire Alpine domain (cf.
505 Fig. 1).

506 **2.6 Bias ~~correction~~adjustment approach**

507 Previous work has revealed partly substantial temperature and precipitation biases of the EURO-
508 CORDEX RCMs over the Alps (e.g. Kotlarski et al., 2014; Smiatek et al., 2016), and one has to expect
509 that the separated snowfall amounts are biased too. This would especially hamper the interpretation of
510 absolute climate change signals of the considered snow indices. We therefore explore possibilities to
511 bias-~~adjust~~correct the simulated snowfall amounts and to directly integrate this bias ~~correction~~
512 adjustment into the snowfall separation framework of Section 2.5. Note that we deliberately employ the
513 term *bias adjustment* as opposed to *bias correction* to make clear that only certain aspects of the
514 snowfall climate are adjusted and that the resulting dataset might be subject to remaining
515 inaccuracies.

516 ~~We compare results with and without employment of the bias correction procedure outlined below.~~ A
517 simple two-step approach that separately accounts for precipitation and temperature biases and their
518 respective influence on snowfall is chosen. The separate consideration of temperature and
519 precipitation biases allows for a more physically-based bias adjustment of snowfall amounts: Due to
520 the temperature dependency of snowfall occurrence, snowfall biases of a given climate model cannot
521 be expected to remain constant under current and future (i.e., warmer) climate conditions. For
522 instance, a climate model with a given temperature bias might pass the snow-rain temperature
523 threshold earlier or later than reality during the general warming process. Hence, traditional bias
524 adjustment approaches based only on a comparison of observed and simulated snowfall amounts in
525 the historical climate would possibly fail due to a non-stationary bias structure. The bias ~~correction~~
526 adjustment is calibrated in the EVAL period for each individual GCM-RCM chain and over the region of
527 Switzerland, and is then applied to both the CTRL and SCEN period of each chain and for the entire
528 Alpine domain. To be consistent in terms of horizontal grid spacing, the observational data sets
529 RhiresD and TabsD (see Sec. 2.1) are conservatively regridded to the RCM resolution beforehand.

530 In a first step, total simulated precipitation was adjusted by introducing an elevation-dependent
531 ~~correction~~adjustment factor which ~~corrects for~~adjusts precipitation biases regardless of temperature.
532 For this purpose, mean precipitation ratios (RCM simulation divided by observational analysis) for 250
533 m elevation intervals were calculated (Fig. S2). An almost linear relationship of these ratios with
534 elevation was found. Thus, a linear regression between the intervals from 250 m a.s.l. to 2750 m a.s.l.
535 was used for each model chain separately to estimate a robust ~~correction~~adjustment factor. As the
536 number of both RCM grid points and measurement stations at very high elevations (>2750 m a.s.l.) is
537 small (see Sec. 2.1) and biases are subject to a considerable sampling uncertainty, these elevations
538 were not considered in the regression. Overall the fits are surprisingly precise except for the altitude

539 bins above 2000 m (Fig. S2). The precipitation adjustment factors (P_{AF}) for a given elevation were then
540 obtained as the inverse of the fitted precipitation ratios. Multiplying simulated precipitation P with P_{AF}
541 for the respective model chain and elevation results in the ~~corrected-adjusted~~ precipitation:

$$542 \quad P_{\text{corr-adj}} = P \cdot P_{AF} \quad (8)$$

543 For a given GCM-RCM chain and for each elevation interval, the spatially and temporally averaged
544 corrected total precipitation $P_{\text{corr-}P_{\text{adj}}}$ approximately corresponds to the observation-based estimate in
545 the EVAL period.

546 In the second step of the bias ~~adjustment~~correction procedure, temperature biases are accounted
547 for. For this purpose the initial snow fractionation temperature $T^*=2^\circ\text{C}$ of the Richards separation
548 method (see Sec 2.5) is shifted to the value T_a^* for which the spatially (Swiss domain) and temporally
549 (September to May) averaged simulated snowfall amounts for elevations below 2750 m a.s.l. match
550 the respective observation-based reference (see above). Compared to the adjustment of total
551 precipitation, T_a^* is chosen independent of elevation, but separately for each GCM-RCM chain, in
552 order to avoid overparameterization and to not over-interpret the elevation dependency of mean
553 snowfall in the snowfall reference grid. After this second step of the bias ~~adjustment~~correction, the
554 spatially ~~(Swiss domain)~~ and temporally ~~(September to May)~~ averaged simulated snowfall amounts
555 below 2750 m a.s.l. by definition match the reference by definition. Hence, the employed simple bias
556 ~~adjustment correction~~ procedure ~~corrects-adjusts~~ domain-mean snowfall biases averaged over the
557 entire season from September to May. It does, however, not correct for biases in the spatial snowfall
558 pattern, in the seasonal cycle, or in the temporal distribution of daily values. Note that, as the
559 underlying high-resolution data sets are available over Switzerland only, the calibration of the bias
560 ~~correction-adjustment~~ methodology is correspondingly restricted, but the ~~correction-adjustment~~ is then
561 applied to the whole Alpine domain. This approach is justified as elevation-dependent mean winter
562 precipitation and temperature biases of the RCMs employed – assessed by comparison against the
563 coarser-resolved EOBS reference dataset (Haylock et al., 2008) - are very similar ~~for over~~ Switzerland
564 and ~~for over~~ the entire Alpine analysis domain (Figs. S3 and S4).

565 **3 Evaluation**

566 **3.1 RCM raw snowfall**

567 We first carry out an illustrative comparison of RCM raw snowfall amounts (for those simulations only
568 that directly provide snowfall flux) against station observations of snowfall, in order to determine
569 whether the simulated RCM snowfall climate contains valid information despite systematic biases. To
570 this end, simulated raw snowfall amounts of nine EURO-CORDEX simulations (see Tab. 1) averaged
571 over 250 m-elevation intervals and over in the range 950 – 1650 m a.s.l. are compared against
572 observations ~~derived from of~~ measured fresh snow sums from 29 MeteoSwiss stations (see Section
573 2.1), with data available for at least 80% of the EVAL period. For this purpose a mean snow density of
574 100 kg/m^3 for the conversion from measured snow height-depth to water equivalent is assumed. Note
575 that this simple validation is subject to considerable uncertainties as it does not explicitly correct for the

576 scale and elevation gap between grid-cell based RCM output and single-site observations. Especially
577 in complex terrain and for exposed sites, point measurements of snow depth might be non-
578 representative for larger-scale conditions (e.g., Grünewald and Lehning, 2015). Also, the conversion
579 from snow depth to snow water equivalent is of approximate nature only, and fresh snow sums might
580 furthermore misrepresent true snowfall in case that snow melt or snow drift occurs between two snow
581 depth readings.

582 At low elevations simulated mean September-May raw snowfall sums match the observations well
583 while differences are larger aloft (Fig. 3a). The positive bias at high elevations might arise from the fact
584 that (the very few) observations were made at ~~a~~ specific locations while simulated grid point values of
585 the corresponding elevation interval might be located in different areas of Switzerland. It might also be
586 explained by positive RCM precipitation and negative RCM temperature biases at high elevations of
587 the Alps (e.g., Kotlarski et al., 2015). At lower elevations, the station network is geographically more
588 balanced and the observations are probably more representative of the respective elevation interval.
589 Despite a clear positive snowfall bias in mid-winter, the RCMs are generally able to reproduce the
590 mean seasonal cycle of snowfall for elevations between 950 m a.s.l. - 1650 m a.s.l. (Fig. 3b). The fact
591 that the major patterns of both the snowfall-elevation relationship and the mean seasonal snowfall
592 cycle are basically well represented indicates the general and physically consistent applicability of
593 RCM output to assess future changes in mean and heavy Alpine snowfall. However, substantial
594 biases in snowfall amounts are apparent and a bias ~~correction~~ adjustment of simulated snowfall
595 seems to be required prior to the analysis of climate change signals of individual snowfall indices.

596 **3.2 Evaluation of the reference snowfall**

597 The snowfall separation employing the Richards method (Section 2.5) and, as a consequence, also
598 the bias adjustment (Section 2.6) make use of the 2 km reference snowfall grid derived by employing
599 the Subgrid method on the observed temperature and precipitation grids. Hence, the final results of
600 this study could to some extent be influenced by inaccuracies and uncertainties of the reference
601 snowfall grid itself. In order to assess the quality of the latter and in absence of a further observation-
602 based reference we here present an approximate evaluation.

603 First, the reference snowfall grid is evaluated against fresh snow sums at the 29 Swiss stations that
604 were also used for evaluating RCM raw snowfall. Note the limitations of such a comparison as outlined
605 in Chapter 3.1. The comparison of black and red markers and lines in Figure 3 indicates a good
606 agreement of mean snowfall at individual elevation intervals (left panel) as well for the mean annual
607 cycle of snowfall at medium elevations (right panel). The reference snowfall grid is obviously a good
608 approximation of site-scale fresh snow sums. Note that similarly to the RCM raw snowfall evaluation,
609 all 2 km reference snowfall grid cells in the respective elevation interval are considered. The good
610 agreement, however, still holds if only those 2 km grid cells covering the 29 site locations are
611 considered (not shown here).

612 Second, both the 2 km reference snowfall grid and the 0.11° reference snowfall grid obtained by
613 employing the Richards method to aggregated temperature and precipitation values (see Section 2.5)
614 are compared against the gridded HISTALP dataset of solid precipitation (Chimani et al., 2011). The

615 latter is provided at a monthly resolution on a 5' grid covering the Greater Alpine Region. It is based on
616 monthly snowfall fraction estimates that are used to scale a gridded dataset of total precipitation. The
617 comparison of the three datasets for the region of Switzerland (for which the 2 km reference snowfall
618 is available) in the EVAL period 1971-2005 yields an approximate agreement of both the magnitude of
619 mean winter snowfall and its spatial pattern. The three data sets differ with respect to their spatial
620 resolution but all show a clear dependency of snowfall on topography and mean September-May
621 snowfall sums above 1000 mm over most parts of the Alpine ridge. Climatologically warm and dry
622 valleys, on the other hand, are represented by minor snowfall amounts of less than 400 m only.

623 As mentioned before these evaluations of the reference snowfall grid are subject to uncertainties and,
624 furthermore, they only cover mean snowfall amounts. However, they provide basic confidence in the
625 applicability of the reference snowfall grid for the purposes of snowfall separation and bias adjustment
626 in the frame of the present study.

627

628 **3.32 Calibration of bias ~~correction~~-adjustment**

629 The analysis of total precipitation ratios (RCM simulations with respect to observations) for the EVAL
630 period, which are computed to carry out the first step of the bias ~~correction~~-adjustment procedure,
631 reveals substantial elevation dependencies. All simulations tend to overestimate total precipitation at
632 high elevations (Fig. S24). This fact might ultimately be connected to an overestimation of surface
633 snow amount in several EURO-CORDEX RCMs as reported by Terzago et al. (2017). As the
634 precipitation ratio between simulations and observations depends approximately linearly ~~depends~~-on
635 elevation, the calculation of P_{AF} via a linear regression of the ratios against elevation (see Sec. 2.6)
636 seems reasonable. By taking the inverse of this linear relation, P_{AF} for every model and elevation can
637 be derived. For the CCLM and RACMO simulations, these correction factors do not vary much with
638 height, while P_{AF} for MPI-ESM - REMO and EC-EARTH - HIRHAM is much larger than 1 in low lying
639 areas, indicating a substantial underestimation of observed precipitation sums (Fig. 4a). However, for
640 most elevations and simulations, P_{AF} is generally smaller than 1, i.e., total precipitation is
641 overestimated by the models. Similar model biases in the winter and spring seasons have already
642 been reported in previous works (e.g., Rajczak et al., in prep.; Smiatek et al., 2016). Especially at high
643 elevations, these apparent positive precipitation biases could be related to observational undercatch,
644 i.e., an underestimation of true precipitation sums by the observational analysis. Frei et al. (2003)
645 estimated seasonal Alpine precipitation undercatch for three elevation intervals. Results show that
646 measurement biases are largest in winter and increase with altitude. However, a potential undercatch
647 (with a maximum of around 40% at high elevations in winter; Frei et al., 2003) can only partly explain
648 the partly substantial overestimation of precipitation found in the present work.

649 After applying P_{AF} to the daily precipitation fields, a snowfall fractionation at the initial T^* of 2 °C (see
650 Eq. (4)) would lead to a snowfall excess in all 14 simulations as models typically experience a cold
651 winter temperature bias. To match the observation-based and spatio-temporally averaged reference
652 snowfall below 2750 m a.s.l., T^* for all models needs to be decreased during the second step of the
653 bias ~~correction~~-adjustment (Fig 4b). The adjusted T_a^* values indicate a clear positive relation with the

654 mean temperature bias in the EVAL period. This feature is expected since the stronger a particular
655 model's cold bias the stronger the required adjustment of the snow fractionation temperature T^*
656 towards lower values in order to avoid a positive snowfall bias. Various reasons for the scatter around
657 a simple linear relation in Figure 4b can be thought of. These include remaining spatial inaccuracies of
658 the corrected precipitation grid, elevation-dependent temperature biases and misrepresented
659 temperature-precipitation relationships at daily scale. Note that precipitation and temperature biases
660 heavily depend on the GCM-RCM chain and seem to be rather independent from each other. While
661 EC-EARTH – RACMO, for instance, shows one of the best performances in terms of total
662 precipitation, its temperature bias of close to -5 °C is the largest deviation in our set of simulations.
663 Concerning the partly substantial temperature biases of the EURO-CORDEX models shown in Figure
664 4 b, their magnitude largely agrees with Kotlarski et al. (2014; in reanalysis-driven simulations) and
665 Smiatek et al. (2016).

666 **3.43 Evaluation of snowfall indices**

667 We next assess the performance of the bias correction-adjustment procedure by comparing snowfall
668 indices derived from separated and bias-corrected-adjusted RCM snowfall amounts against the
669 observation-based reference. The period for which this comparison is carried out is EVAL, i.e., it is
670 identical to the calibration period of the bias correction-adjustment. We hence do not intend a classical
671 cross validation exercise with separate calibration and validation periods, but try to answer the
672 following two questions: (a) Which aspects of the Alpine snowfall climate are corrected-for-adjusted,
673 and (b) for which aspects do biases remain even after application of the bias correction-adjustment
674 procedure.

675 Figure 5 shows the evaluation results of the six snowfall indices based on the separated and not bias-
676 corrected-adjusted simulated snowfall ($RCM_{sep+nb_{ae}}$), and the separated and bias-corrected-adjusted
677 simulated snowfall ($RCM_{sep+b_{ae}}$). In the first case the snowfall separation of raw precipitation is
678 performed with $T^*=2^{\circ}C$, while in the second case precipitation is corrected-adjusted and the separation
679 is performed with a bias-adjusted temperature T^*_a . The first column represents the mean September
680 to May statistics, while columns 2-4 depict the seasonal cycle at monthly resolution for three distinct
681 elevation intervals.

682 The analysis of S_{mean} confirms that $RCM_{sep+b_{ae}}$ is able to reproduce the observation-based reference in
683 the domain mean as well as in most individual elevation intervals. The domain-mean agreement is a
684 direct consequence of the design of the bias correction-adjustment procedure (see above).
685 $RCM_{sep+nb_{ae}}$, on the other hand, consistently overestimates S_{mean} by up to a factor of 2.5 as a
686 consequence of positive precipitation and negative temperature biases (cf. Fig. 4). Also the seasonal
687 cycle of S_{mean} for $RCM_{sep+b_{ae}}$ yields a satisfying performance across all three elevation intervals, while
688 $RCM_{sep+nb_{ae}}$ tends to produce too much snowfall over all months and reveals an increasing model
689 spread with elevation.

690 For the full domain and elevations around 1000 m, the observation-based reference indicates a mean
691 S_{freq} of 20% between September and May. Up to 1000 m a.s.l. $RCM_{sep+b_{ae}}$ reflects the increase of this

692 index with elevation adequately. However, towards higher elevations the approximately constant S_{freq}
693 of 30% in the reference is not captured by the simulation-derived snowfall. Notably during wintertime,
694 both $\text{RCM}_{\text{sep+b}_{\text{ae}}}$ and $\text{RCM}_{\text{sep+nb}_{\text{ae}}}$ produce too many snowfall days, i.e., overestimate snowfall
695 frequency. This feature is related to the fact that climate models typically tend to overestimate the wet
696 day frequency over the Alps especially in wintertime (Rajczak et al., 2013) and that the bias ~~correction~~
697 adjustment procedure employed does not explicitly correct for potential biases in precipitation
698 frequency. Due to the link between mean snowfall on one side and snowfall frequency and mean
699 intensity on the other side, opposite results are obtained for the mean snowfall intensity S_{int} .
700 $\text{RCM}_{\text{sep+b}_{\text{ae}}}$ largely underestimates mean intensities during snowfall days while $\text{RCM}_{\text{sep+nb}_{\text{ae}}}$ typically
701 better reflects the reference. Nevertheless, deviations during winter months at mid-elevations are not
702 negligible. Mean September-May S_{frac} in the reference exponentially increases with elevation. This
703 behaviour is reproduced by both $\text{RCM}_{\text{sep+b}_{\text{ae}}}$ and $\text{RCM}_{\text{sep+nb}_{\text{ae}}}$. Notwithstanding, $\text{RCM}_{\text{sep+b}_{\text{ae}}}$ results are
704 more accurate compared to $\text{RCM}_{\text{sep+nb}_{\text{ae}}}$, which turns out to be biased towards too large snowfall
705 fractions.

706 For the two heavy snowfall indices S_{q99} and S_{1d} , $\text{RCM}_{\text{sep+nb}_{\text{ae}}}$ appears to typically match the reference
707 better than $\text{RCM}_{\text{sep+b}_{\text{ae}}}$. Especially at high elevations, $\text{RCM}_{\text{sep+b}_{\text{ae}}}$ produces too low snowfall amounts.
708 This again ~~highlights-illustrates~~ the fact that the bias ~~adjustment correction~~ procedure is designed to
709 ~~correct-adjust for~~ biases in mean snowfall, but does not necessarily improve further aspects of the
710 simulated snowfall climate.

711 The spatial patterns of S_{mean} for the 14 $\text{RCM}_{\text{sep+b}_{\text{ae}}}$ simulations from September to May are presented
712 in Figure 6. The observational-based reference (lower right panel) reveals a snowfall distribution with
713 highest values along the Alpine main ridge, whereas the Swiss plateau, Southern Ticino and main
714 valleys such as the Rhône and Rhine valley experience less snowfall. Almost all bias-~~corrected~~
715 adjusted models are able to represent the overall picture with snow-poor lowlands and snow-rich
716 Alpine regions. Nevertheless substantial differences to the observations concerning the spatial
717 snowfall pattern can arise. EC-EARTH - HIRHAM, for example, is subject to a "pixelated" structure.
718 This could be the result of frequent grid-cell storms connected to parameterisations struggling with
719 complex topographies. Such inaccuracies in the spatial pattern are not corrected for by our simple bias
720 ~~correction-adjustment~~ approach ~~which that~~ only targets domain-mean snowfall amounts at elevations
721 below 2750 m a.s.l. and that does not considerably modify the simulated spatial snowfall patterns..
722 Note that these patterns are obviously strongly determined by the RCM itself and only slightly depend
723 on the driving GCM (see, for instance, the good agreement among the CCLM and the RCA
724 simulations).

725 In summary, after applying the bias ~~adjustment correction~~ to the simulations most snowfall indices are
726 fairly well represented at elevations below 1000 m a.s.l.. With increasing altitude and smaller sample
727 sizes in terms of number of grid cells, reference and $\text{RCM}_{\text{sep+b}_{\text{ae}}}$ diverge. This might be caused by the
728 remaining simulated overestimation of S_{freq} and an underestimation of S_{int} . While the bias adjustment
729 ~~correction~~ approach leads to a reduction of S_{int} due to the total precipitation adjustment, S_{freq} is only
730 slightly modified by this correction and by the adjustment of T^* . Nevertheless, these two parameters

731 strongly influence other snowfall indices. The counteracting effects of overestimated S_{freq} and
732 underestimated S_{int} result in appropriate amounts of S_{mean} whereas discrepancies for S_{q99} and S_{1d} are
733 mainly driven by the underestimation of S_{int} .

734 **4 Snowfall projections for the late 21st century**

735 For the study of climate change signals, the analysis domain is extended to the entire Alps (see Sec.
736 2.3). Due to the identified difficulties of bias-~~correcting-adjusting~~ certain snowfall indices (see Sec
737 3.43), emphasis is laid upon relative signals of change (see Eq. 2). This type of change can be
738 expected to be less dependent on the remaining inaccuracies after the ~~correctionadjustment~~. If not
739 stated otherwise, all results in this Section are based on the RCM_{sep+base} data, i.e., on separated and
740 bias-~~corrected-adjusted~~ RCM snowfall, and on the RCP8.5 emission scenario.

741 Projections for seasonal S_{mean} show a considerable decrease over the entire Alpine domain (Fig. 7).
742 Most RCMs project largest percentage losses of more than 80% across the Alpine forelands ~~and~~
743 ~~especially in its topographic depressions~~ such as the Po ~~and Rhone v~~Valleys ~~or Western France~~. Over
744 the Alpine ridge, reductions are smaller but still mostly negative. Elevated regions between
745 Southeastern Switzerland, Northern Italy and Austria seem to be least affected by the overall snowfall
746 reduction. Some of the simulations (e.g., CNRM-RCA, MPI-ESM-RCA or MPI-ESM-REMO) project
747 only minor changes in these regions. Experiments employing the same RCM but different driving
748 GCMs (e.g. the four simulations of RCA), but also experiments employing the same GCM but different
749 RCMs (e.g. the four simulations driven by EC-EARTH, ~~though different realizations~~) can significantly
750 disagree in regional-scale change patterns and especially in the general magnitude of change. This
751 highlights a strong influence of both the driving GCMs and the RCMs themselves on snowfall changes,
752 representing effects of ~~large-scale~~ circulation and meso-scale response, respectively.

753 A more detailed analysis is provided in Fig. 8 ~~that-which~~ addresses the vertical and seasonal
754 distribution of snowfall changes. It reveals that relative (seasonal mean) changes of S_{mean} appear to be
755 strongly dependent on elevation (Fig.8, top left panel). The multi-~~model~~ mean change ranges from -
756 80% at low elevations to -10% above 3000 m a.s.l.. Largest differences between neighbouring
757 elevation intervals are obtained from 750 m a.s.l. to 1500 m a.s.l.. Over the entire Alps, the results
758 show a reduction of S_{mean} by -35% to -55% with a multi-~~model~~ mean of -45%. The multi-~~model~~ spread
759 appears to be rather independent of elevation and is comparably small, confirming that, overall, the
760 spatial distributions of the change patterns are similar across all model chains (cf. Fig. 7). All
761 simulations point to decreases over the entire nine-month period September to May for the two
762 elevation intervals <1000 m a.s.l. and 1000 to 2000 m a.s.l.. Above 2000 m a.s.l., individual
763 simulations show an increase of S_{mean} by up to 20% in mid-winter which ~~forces-the-leads to a slightly~~
764 ~~positive change in~~ multi-~~model~~ mean ~~change-to-be-slightly-positive~~ in January and February.

765 Decreases of S_{freq} are very similar to change-s_{in} mean snowfall. Mean September-May changes are
766 largest below 1000 m a.s.l., while differences among elevation intervals become smaller ~~in-the-upper~~
767 ~~partat higher elevations~~. In-between is a transition zone with rather strong changes with elevation,
768 ~~which approximately corresponds to the mean elevation of the September-May zero-degree line in~~

769 | [today's climate \(e.g., Ceppi et al., 2012; MeteoSchweiz, 2016\)](#). Individual simulations with large
770 reductions in S_{mean} , such as the RCA experiments, also project strongest declines in S_{freq} . In contrast,
771 the mean snowfall intensity S_{int} is subject to smallest percentage variations in our set of snowfall
772 indices. Strong percentage changes for some models in September are due to the small sample size
773 (only few grid points considered) and the low snowfall amounts in this month. Apart from mid
774 elevations with decreases of roughly -10%, mean intensities from September to May are projected to
775 remain almost unchanged by the end of the century. For both seasonal and monthly changes, model
776 | agreement is best for high elevations while the multi-model spread is largest for lowlands. Large model
777 spread at low elevations might be caused by the small number of grid points used for averaging over
778 the respective elevation interval, especially in autumn and spring.

779 Similar results are obtained for the heavy snowfall indices S_{q99} and S_{1d} . While percentage decreases
780 at lowermost elevations are even larger than for S_{mean} , losses at high elevations are less pronounced,
781 resulting in similar domain-mean change signals for heavy and mean snowfall. Substantial differences
782 between monthly δS_{q99} and δS_{1d} appear at elevations below 1000 m a.s.l.. Here, percentage losses of
783 S_{q99} are typically slightly more pronounced. Above 2000 m a.s.l. both indices appear to remain almost
784 | constant between January and March with change signals close to zero. The multi-model mean
785 changes even hint to slight increases of both indices. Concerning changes in the snowfall fraction, i.e.,
786 in the relative contribution of snowfall to total precipitation, our results indicate that current seasonal
787 and domain mean S_{frac} might drop by about -50% (Fig. 8, lowermost row). Below 1000 m a.s.l., the
788 | strength of the signal is almost independent of the month, and multi-model average changes of the
789 snow fraction of about -80% are obtained. At higher elevations changes during mid-winter are less
790 pronounced compared to autumn and spring but still negative.

791 **5 Discussion**

792 **5.1 Effect of temperature, snowfall frequency and intensity on snowfall changes**

793 The results in Section 4 indicate substantial changes of snowfall indices over the Alps in regional
794 climate projections. With complementary analyses presented in Figures 9 and 10 we shed more light
795 on the responsible mechanisms, especially concerning projected changes in mean and heavy
796 snowfall. For this purpose Figures 9a-b,e-f show the relationship of both mean and heavy snowfall
797 amounts in the CTRL period and their respective percentage changes with the climatological CTRL
798 temperature of the respective (climatological) month, elevation interval and GCM-RCM chain. For
799 absolute amounts (S_{mean} , S_{q99} ; Fig. 9a,e) a clear negative relation is found, i.e., the higher the CTRL
800 temperature the lower the snowfall amounts. For S_{mean} the relation levels off at mean temperatures
801 higher than about 6°C with mean snowfall amounts close to zero. For temperatures below about -6°C
802 a considerable spread in snowfall amounts is obtained, i.e., mean temperature does not seem to be
803 the controlling factor here. Relative changes of both quantities (Fig. 9b,f), however, are strongly
804 controlled by the CTRL period's temperature level with losses close to 100% for warm climatic settings
805 and partly increasing snowfall amounts for colder climates. This dependency of relative snowfall
806 changes on CTRL temperature is in line with previous works addressing future snowfall changes on

807 both hemispheric and regional scales (de Vries et al., 2014; Krasting et al., 2013; Räisänen, 2016).
808 The spread of changes within a given CTRL temperature bin can presumably be explained by the
809 respective warming magnitudes that differ between elevations, months and GCM-RCM chains. About
810 half of this spread can be attributed to the month and the elevation alone (compare the spread of the
811 black markers to the one of the red markers which indicate multi-model averages).

812 For most months and elevation intervals, percentage reductions in S_{mean} and S_{q99} reveal an almost
813 linear relationship with δS_{freq} (Fig. 9c, g). The decrease of S_{freq} with future warming can be explained
814 by a shift of the temperature probability distribution towards higher temperatures, leading to fewer
815 days below the freezing level (Fig. 10, top row). Across the three elevation intervals <1000 m a.s.l.,
816 1000-2000 m a.s.l. and > 2000 m a.s.l., relative changes in the number of days with temperatures
817 below the freezing level ($T \leq 0^\circ\text{C}$) are in the order of -65%, -40% and -20%, respectively (not shown).
818 This approximately corresponds to the simulated decrease of S_{freq} (cf. Fig 8), which in turn, is of a
819 similar magnitude as found in previous works addressing future snowfall changes in the Alps
820 (Schmucki et al., 2015b; Zubler et al., 2014). Due to the general shift of the temperature distribution
821 and the “loss” of very cold days (Fig. 10, top row) future snowfall furthermore occurs in a narrower
822 temperature range (Fig. 10, second row).

823 Contrasting this general pattern of frequency-driven decreases of both mean and heavy snowfall, no
824 changes or even slight increases of S_{mean} , S_{q99} and S_{1d} at high elevations are expected in mid-winter
825 (see Fig. 8). This can to some part be explained by the general increase of total winter precipitation
826 (Rajczak et al., in prep; Smiatek et al., 2016) that obviously offsets the warming effect in high-elevation
827 regions where a substantial fraction of the future temperature PDF is still located below the rain-snow
828 transition (Fig. 10, top row). This process has also been identified in previous works to be, at last
829 partly, responsible for future snowfall increases (de Vries et al., 2014; Krasting et al., 2013; Räisänen,
830 2016). Furthermore, the magnitude of the increases of both mean and heavy snowfall is obviously
831 driven by positive changes of S_{int} , while S_{freq} remains constant (Fig. 9c,g). An almost linear relationship
832 between positive changes of S_{int} and positive changes of S_{mean} and S_{q99} is obtained (Fig. 9d,h; upper
833 right quadrants). Nevertheless, the high-elevation mid-winter growth in S_{mean} is smaller than the
834 identified increases of mean winter total precipitation. This can be explained by the persistent
835 decrease of S_{frac} during the cold season (see Fig. 8, lowermost row).

836 For elevation intervals with simulated monthly temperatures between -6°C and 0°C in the CTRL
837 period, S_{mean} appears to decrease stronger than S_{q99} (cf. Fig. 9b,f). O’Gorman (2014) found a very
838 similar behaviour when analysing mean and extreme snowfall projections over the Northern
839 Hemisphere within a set of GCMs. This finding is related to the fact that future snowfall decreases are
840 mainly governed by a decrease of snowfall frequency while snowfall increases in high-elevated
841 regions in mid-winter seem to be caused by increases of snowfall intensity. It can obviously be
842 explained by the insensitivity of the temperature interval at which extreme snowfall occurs to climate
843 warming and by the shape of the temperature – snowfall intensity distribution itself (Fig. 10, third row).
844 The likely reason behind positive changes of S_{int} at high-elevated and cold regions is the higher water
845 holding capacity of the atmosphere in a warmer climate. According to the Clausius-Clapeyron relation,

846 saturation vapour pressure increases by about 7% per degree warming (Held and Soden, 2006).
847 Previous studies have shown that simulated changes of heavy and extreme precipitation (though not
848 necessarily targeting the daily temporal scale and moderate extremes as in our case) are consistent
849 with this theory (e.g., Allen and Ingram, 2002; Ban et al., 2015). In terms of snowfall, we find the
850 Clausius-Clapeyron relation to be applicable for negative temperatures up to approximately -5°C as
851 well (Fig. 10, third row, dashed lines). Inconsistencies for temperatures between -5°C and 0°C are due
852 to a snow fraction $sf < 100\%$ for corresponding precipitation events.

853 For further clarification, Figure 11 schematically illustrates the governing processes behind the
854 changes of mean and heavy snowfall that differ between climatologically warm (decreasing snowfall)
855 and climatologically cold climates (increasing snowfall). As shown in Figure 10 (third row), the mean
856 S_{int} distribution is rather independent on future warming and similar temperatures are associated with
857 similar mean snowfall intensities. In particular, heaviest snowfall is expected to occur slightly below the
858 freezing level in both the CTRL and the SCEN period (Fig. 11a). How often do such conditions prevail
859 in the two periods? In a warm current climate, i.e., at low elevations or in the transition seasons, heavy
860 snowfall only rarely occurs as the temperature interval for highest snowfall intensity is already situated
861 in the left tail of the CTRL period's temperature distribution (Fig. 11b). With future warming, i.e., with a
862 shift of the temperature distribution to the right, the probability for days to occur in the heavy snowfall
863 temperature interval (dark grey shading) decreases stronger than the probability of days to occur in
864 the overall snowfall regime (light grey shading). This results in (1) a general decrease of snowfall
865 frequency, (2) a general decrease of mean snowfall intensity and (3) a general and similar decrease of
866 both mean and heavy snowfall amounts. In contrast, at cold and high-elevated sites CTRL period
867 temperatures are often too low to trigger heavy snowfall since a substantial fraction of the temperature
868 PDF is located to the left of the heavy snowfall temperature interval (Fig. 11 c). The shifted distribution
869 in a warmer SCEN climate, however, peaks within the temperature interval that favours heavy
870 snowfall. This leads to a probability increase for days to occur in the heavy snowfall temperature range
871 despite the general reduction in S_{freq} (lower overall probability of days to occur in the entire snowfall
872 regime, light grey). As a consequence, mean S_{int} tends to increase and the reduction of heavy
873 snowfall amounts is less pronounced (or even of opposing sign) than the reduction in mean snowfall.
874 For individual (climatologically cold) regions and seasons, the increase of mean S_{int} might even
875 compensate the S_{freq} decrease, resulting in an increase of both mean and heavy snowfall amounts.
876 Note that in a strict sense these explanations only hold in the case that the probability of snowfall to
877 occur at a given temperature does not change considerably between the CTRL and the SCEN period.
878 This behaviour is approximately given-found (Fig. 10, bottom row), which presumably indicates only
879 minor contributions of large scale circulation changes and associated humidity changes on both the
880 temperature - snowfall frequency and the temperature - snowfall intensity relation.

881 5.2 Emission scenario uncertainty

882 The projections presented in the previous sections are based on the RCP8.5 emission scenario, but
883 will depend on the specific emission-scenario considered. To assess this type of uncertainty we here
884 compare the RCM_{sep+b_{ae}} simulations for the previously shown RCP8.5 emission scenario against those
885 assuming the more moderate RCP4.5 scenario. As a general picture, the weaker RCP4.5 scenario is

886 associated with less pronounced changes of snowfall indices (Fig. 12). Differences in mean seasonal
 887 δS_{mean} between the two emission scenarios are most pronounced below 1000 m a.s.l. where
 888 percentage changes for RCP4.5 are about one third smaller than for RCP8.5. At higher elevations,
 889 multi-model mean changes better agree and the multi-model ranges for the two emission scenarios
 890 start overlapping, i.e., individual RCP4.5 experiments can be located in the RCP8.5 multi-model range
 891 and vice versa. Over the entire Alpine domain, about -25% of current snowfall is expected to be lost
 892 under the moderate RCP4.5 emission scenario while a reduction of approximately -45% is projected
 893 for RCP8.5. For seasonal cycles, the difference of δS_{mean} between RCP4.5 and RCP8.5 is similar for
 894 most months and slightly decreases with altitude. Above 2000 m a.s.l., the simulated increase of S_{mean}
 895 appears to be independent of the chosen RCP in January and February, while negative changes
 896 before and after mid-winter are more pronounced for RCP8.5. Alpine domain mean δS_{q99} almost
 897 doubles under the assumption of stronger GHG emissions. This is mainly due to differences at low
 898 elevations whereas above 2000 m a.s.l. δS_{q99} does not seem to be strongly affected by the choice of
 899 the emission scenario. Differences in monthly mean changes are in close analogy to δS_{mean} . Higher
 900 emissions lead to a further negative shift in δS_{q99} . Up to mid-elevations differences are rather
 901 independent of the season. However, at highest elevations and from January to March, differences
 902 between RCP4.5 and RCP8.5 are very small.

903 Despite the close agreement of mid-winter snowfall increases at high elevations between the two
 904 emission scenarios, obvious differences in the spatial extent of the region of mean seasonal snowfall
 905 increases can be found (cf Figs. S65 and 7 for δS_{mean} , and Figs. S76 and S87 for δS_{q99}). In most
 906 simulations, the number of grid cells along the main Alpine ridge that show either little change or even
 907 increases of seasonal mean S_{mean} or S_{q99} is larger for RCP4.5 than for RCP8.5 with its larger warming
 908 magnitude.

909 5.3 Intercomparison of projections with separated and raw snowfall

910 The snowfall projections presented above are based on the RCM_{sep+ba} data set, i.e. on separated and
 911 bias-adjusted snowfall amounts. To assess the robustness of these estimates we here compare the
 912 obtained change signals against the respective signals based on ~~An intercomparison of relative~~
 913 ~~change signals for RCM_{sep+bc} (separated and bias-corrected), RCM_{sep+nbae} (separated and not bias-~~
 914 ~~corrected/adjusted) and simulated raw snowfall output (RCM_{raw}).~~ based on ~~This comparison is~~
 915 restricted to the nine RCMs providing raw snowfall as output variable (see Tab. 1).

916 The three different change estimates agree well with each other In terms of relative snowfall change
 917 signals reveals no substantial differences (Fig. 13, top row). ~~In the three data sets, m~~Multi-model mean
 918 relative changes are very similar for all analysed snowfall indices and elevation intervals. In many
 919 cases, separated and not bias-adjusted snowfall (RCM_{sep+nba}) is subject to slightly smaller percentage
 920 decreases. Furthermore, mMulti-model mean differences between RCM_{sep+bae}, RCM_{sep+nbae} and
 921 RCM_{raw} simulations are smaller than the corresponding multi-model spread of RCM_{sep+bae} simulations
 922 and emission scenario uncertainties (cf. Figs. 12, 13 and S108).

923 This ~~agreement in terms of relative change signals finding~~ is in contrast to absolute change
924 characteristics (Fig. 13, bottom row). Results based on the three data sets agree in the sign of change,
925 but not in their magnitude, especially at high elevations >2000 m a.s.l.. As the relative changes are
926 almost identical, the absolute changes strongly depend upon the treatment of biases in the control
927 climate.

928 -In summary, these findings indicate that (a) the snowfall separation method developed in the present
929 work yields rather good proxies for relative changes of snowfall indices in raw RCM output (which is
930 ~~not available for all for many~~ GCM-RCM chains ~~not available~~), and that (b) the additional bias ~~-~~
931 ~~adjustment correction~~ of separated snowfall amounts only has a weak influence on relative change
932 signals of snowfall indices, but can have substantial effects on absolute changes.

933 **6 Conclusions and outlook**

934 The present work makes use of state-of-the-art EURO-CORDEX RCM simulations to assess changes
935 of snowfall indices over the European Alps by the end of the 21st century. For this purpose, snowfall is
936 separated from total precipitation using near-surface air temperature in both the RCMs and in the an
937 observation-based estimates on a daily basis. The analysis yields a number of robust signals,
938 consistent across a range of climate model chains and across emission scenarios. Relating to the
939 main objectives we find the following:

940 **Snowfall separation on an RCM grid.** Binary snow fractionation with a fixed temperature threshold
941 on coarse-resolution grids (with 11 km resolution) leads to an underestimation of mean snowfall and
942 an overestimation of heavy snowfall. To overcome these deficiencies, the Richards snow fractionation
943 method is implemented. This approach expresses that the coarse-grid snow fraction depends not only
944 on daily mean temperature, but also on topographical subgrid-scale variations. Accounting for the
945 latter results in better estimates for mean and heavy snowfall. However, due to limited observational
946 coverage the parameters of this method are fitted for Switzerland only and are then applied to the
947 entire Alpine domain. Whether this spatial transfer is robust could further be investigated by using
948 observational data sets covering the full domain of interest but is out of the scope of this study.

949 **Snowfall bias ~~correction~~ adjustment.** Simulations of the current EURO-CORDEX ensemble are
950 subject to considerable biases in precipitation and temperature, which translate into biased snowfall
951 amounts. In the EVAL period, simulated precipitation is largely overestimated, with increasing biases
952 toward higher altitudes. On the other hand, simulated near surface temperatures are generally too low
953 with largest deviations over mountainous regions. These findings were already reported in previous
954 studies for both the current EURO-CORDEX data set but also for previous RCM ensembles (e.g. Frei
955 et al., 2003; Kotlarski et al., 2012; Kotlarski et al., 2015; Rajczak et al., 2013; Smiatek et al., 2016). By
956 implementing a simple bias ~~adjustment~~ correction approach, we are able to partly reduce these biases
957 and the associated model spread, which should enable more robust change estimates. The corrected
958 adjusted model results reproduce the seasonal cycles of mean snowfall fairly well. However,
959 substantial biases remain in terms of heavy snowfall, snowfall intensities (which in general are
960 overestimated), snowfall frequencies, and spatial snowfall distributions. Further improvements might

961 | be feasible by using more sophisticated bias ~~adjustment correction~~ methods, such as quantile
962 | mapping (e.g., Rajczak et al., 2016), local intensity scaling of precipitation (e.g., Schmidli et al., 2006),
963 | or weather generators (e.g. Keller et al., 2016). Advantages of the approach employed here are its
964 | simplicity, its direct linkage to the snowfall separation method and, as a consequence, its potential
965 | ability to account for non-stationary snowfall biases. Furthermore, a comparison to simulated raw
966 | snowfall for a subset of nine simulations revealed that relative change signals are almost independent
967 | of the chosen post-processing strategy.

968 | **Snowfall projections for the late 21st century.** Snowfall climate change signals are assessed by
969 | deriving the changes in snowfall indices between the CTRL period 1981 - 2010 and the SCEN period
970 | 2070 - 2099. Our results show that by the end of the 21st century, snowfall over the Alps will be
971 | considerably reduced. Between September and May mean snowfall is expected to decrease by
972 | approximately -45% (multi-model mean) under an RCP8.5 emission scenario. For the more moderate
973 | RCP4.5 scenario, multi-model mean projections show a decline of -25%. These results are in good
974 | agreement with previous works (e.g. de Vries et al., 2014; Piazza et al., 2014, Räisänen, 2016). Low-
975 | lying areas experience the largest percentage changes of more than -80%, while the highest Alpine
976 | regions are only weakly affected. Variations of heavy snowfall, defined by the 99% all-day snowfall
977 | percentile, show ~~at low-lying elevations~~ an even more pronounced signal at low-lying elevations. With
978 | increasing elevation, percentage changes of heavy snowfall are generally smaller than for mean
979 | snowfall. O'Gorman (2014) found a very similar behaviour by analysing projected changes in mean
980 | and extreme snowfall over the entire Northern Hemisphere. He pointed out that heavy and extreme
981 | snowfall occurs near an optimal temperature (near or below freezing, but not too cold), which seems to
982 | be independent of climate warming. We here confirm this ~~conclusion finding~~. At mid and high
983 | elevations ~~the optimal temperature for~~ heavy snowfall in a warmer climate will still occur in ~~a warmer~~
984 | ~~climate the optimal temperature range~~ and, hence, heavy snowfall amounts will decrease less strongly
985 | compared to mean snowfall, and may even increase in some areas.:-

986 | At first approximation, the magnitude of future warming strongly influences the reduction of mean and
987 | heavy snowfall by modifying the snowfall frequency. Snowfall increases may however occur at high
988 | (and thus cold) elevations, and these are not caused by frequency changes. Here, snowfall increases
989 | due to (a) a general increase of total winter precipitation combined with only minor changes in snowfall
990 | frequency, and (b) more intense snowfall. This effect has a pronounced altitudinal distribution and may
991 | be particularly strong under conditions (depending upon location and season) where the current
992 | climate is well below freezing. Such conditions may experience a shift towards a ~~more snowfall-~~
993 | ~~friendly~~ temperature range more favourable to snowfall (near or below freezing, but not too cold) with
994 | corresponding increases of mean snowfall, despite a general decrease of the snowfall fraction.

995 | The identified future changes of snowfall over the Alps can lead to a variety of impacts in different
996 | sectors. With decreasing snowfall frequencies and the general increase of the snowline (e.g.,
997 | Beniston, 2003; Gobiet et al., 2014; Hantel et al., 2012), both associated with temperature changes,
998 | ski lift operators are looking into an uncertain future. A shorter snowfall season will likely put them
999 | under greater financial pressure. Climate change effects might be manageable only for ski areas

1000 reaching up to high elevations (e.g. Elsasser and Bürki, 2002). Even so these resorts might start later
1001 into the ski season, the snow conditions into early spring could change less dramatically due to
1002 projected high-elevation snowfall increases in mid-winter. A positive aspect of the projected decrease
1003 in snowfall frequency might be a reduced expenditures for airport and road safety (e.g., Zubler et al.,
1004 2015).

1005 At lower altitudes, an intensification of winter precipitation, combined with smaller snowfall fractions
1006 (Serquet et al., 2013), increases the flood potential (Beniston, 2012). Snow can act as a buffer by
1007 releasing melt water constantly over a longer period of time. With climate warming, this storage
1008 capacity is lost, and heavy precipitation immediately drains into streams and rivers which might not be
1009 able to take up the vast amount of water fast enough. Less snowmelt will also have impacts on
1010 hydropower generation and water management (e.g., Weingartner et al., 2013). So far, many Alpine
1011 regions are able to bypass dry periods by tapping melt water from mountainous regions. With reduced
1012 snow-packs due to less snowfall, water shortage might become a serious problem in some areas.

1013 Regarding specific socio-economic impacts caused by extreme snowfall events, conclusions based on
1014 the results presented in this study are difficult to draw. It might be possible that the 99% all-day
1015 snowfall percentile we used for defining heavy snowfalls, is not appropriate to speculate about future
1016 evolutions of (very) rare events (Schär et al., 2016). To do so, one might consider applying a
1017 generalized extreme value (GEV) analysis which is more suitable for answering questions related to
1018 rare extreme events.

1019 **7 Data Availability**

1020 The EURO-CORDEX RCM data analysed in the present work are publicly available - parts of
1021 them for non-commercial use only - via the Earth System Grid Federation archive (ESGF;
1022 e.g., <https://esgf-data.dkrz.de>). The observational datasets RHiresD and TabsD as well as
1023 the snow depth data for Switzerland are available for research and educational purposes
1024 from kundendienst@meteoschweiz.ch. The analysis code is available from the
1025 corresponding author on request.

1026 **8 Competing Interests**

1027 The authors declare that they have no conflict of interest.

1028 **9 Acknowledgements**

1029 We gratefully acknowledge the support of Jan Rajczak, Urs Beyerle and Curdin Spirig (ETH Zurich) as
1030 well as Elias Zubler (MeteoSwiss) in data acquisition and pre-processing. Christoph Frei (MeteoSwiss)
1031 and Christoph Marty (WSL-SLF) provided important input on specific aspects of the analysis. [The](#)
1032 [GTOPO30 digital elevation model is available from the U.S. Geological Survey.](#) Finally, we thank the

1033 climate modelling groups of the EURO-CORDEX initiative for producing and making available their
1034 model output.

1035 **10 References**

- 1036 Abegg, B. A., S., Crick, F., and de Montfalcon, A.: Climate change impacts and adaptation in winter tourism, in:
1037 Climate change in the European Alps: adapting winter tourism and natural hazards management, edited by:
1038 Agrawala, S., Organisation for Economic Cooperation and Development (OECD), Paris, France, 25-125, 2007.
- 1039 Allen, M. R., and Ingram, W. J.: Constraints on future changes in climate and the hydrologic cycle, *Nature*, 419,
1040 224-232, 10.1038/nature01092, 2002.
- 1041 Ban, N., Schmidli, J., and Schär, C.: Heavy precipitation in a changing climate: Does short-term summer
1042 precipitation increase faster?, *Geophys Res Lett*, 42, 1165-1172, 10.1002/2014GL062588, 2015.
- 1043 Beniston, M.: Climatic Change in Mountain Regions: A Review of Possible Impacts. *Clim Change*, 59, 5-31.
- 1044 Beniston, M.: Impacts of climatic change on water and associated economic activities in the Swiss Alps, *J Hydrol*,
1045 412, 291-296, 10.1016/j.jhydrol.2010.06.046, 2012.
- 1046 [Ceppi, P., Scherrer, S.C., Fischer, A.M., and Appenzeller, C.: Revisiting Swiss temperature trends 1959–2008, *Int*](#)
1047 [J Climatol](#), 32, 203-213, 10.1002/joc.2260, 2012.
- 1048 CH2011: Swiss Climate Change Scenarios CH2011, published by C2SM, MeteoSwiss, ETH, NCCR Climate, and
1049 OcCC, Zurich, Switzerland, 88 pp, 2011.
- 1050 [Chimani, B., Böhm, R., Matulla, C., and Ganekind, M.: Development of a longterm dataset of solid/liquid](#)
1051 [precipitation, *Adv Sci Res*, 6, 39-43, 10.5194/asr-6-39-2011, 2011.](#)
- 1052 de Vries, H., Haarsma, R. J., Hazeleger, W.: On the future reduction of snowfall in western and central Europe.
1053 *Clim Dyn*, 41, 2319-2330, 10.1007/s00382-012-1583-x, 2013.
- 1054 de Vries, H., Lenderink, G., and van Meijgaard, E.: Future snowfall in western and central Europe projected with a
1055 high-resolution regional climate model ensemble, *Geophys Res Lett*, 41, 4294-4299, 10.1002/2014GL059724,
1056 2014.
- 1057 Deser, C., Knutti, R., Solomon, S. and Phillips, A. S.: Communication of the role of natural variability in future
1058 North American climate. *Nature Clim Change*, 2, 775-779, 2012.
- 1059 Elsasser, H. and Bürki, R.: Climate change as a threat to tourism in the Alps. *Climate Research*, 20, 253-257.
- 1060 Fischer, A. M., Keller, D. E., Liniger, M. A., Rajczak, J., Schär, C., and Appenzeller, C.: Projected changes in
1061 precipitation intensity and frequency in Switzerland: a multi-model perspective, *Int J Climatol*, 35, 3204-3219,
1062 10.1002/joc.4162, 2015.
- 1063 Fischer, E. M. and Knutti, R.: Observed heavy precipitation increase confirms theory and early models. *Nature*
1064 *Clim Change*, 6, 986-992, 10.1038/NCLIMATE3110, 2016.
- 1065 Frei, C. and Schär, C.: A precipitation climatology of the Alps from high-resolution rain-gauge observations, *Int J*
1066 *Climatol*, 18, 873-900, 10.1002/(Sici)1097-0088(19980630)18:8<873::Aid-Joc255>3.0.Co;2-9, 1998.
- 1067 Frei, C., Christensen, J. H., Déqué, M., Jacob, D., Jones, R. G., and Vidale, P. L.: Daily precipitation statistics in
1068 regional climate models: Evaluation and intercomparison for the European Alps, *J Geophys Res-Atmos*, 108,
1069 10.1029/2002jd002287, 2003.
- 1070 Frei, C.: Interpolation of temperature in a mountainous region using nonlinear profiles and non-Euclidean
1071 distances, *Int J Climatol*, 34, 1585-1605, 10.1002/joc.3786, 2014.
- 1072 Giorgi, F.: Simulation of regional climate using a limited area model nested in a general circulation model, *J*
1073 *Climate*, 3, 941-963, 1990.
- 1074 Giorgi, F., Jones, C., and Asrar, G. R.: Addressing climate information needs at the regional level: the CORDEX
1075 framework, *World Meteorological Organization (WMO) Bulletin*, 58, 175, 2009.
- 1076 Giorgi, F., Torma, C., Coppola, E., Ban, N., Schär, C., and Somot, S.: Enhanced summer convective rainfall at
1077 Alpine high elevations in response to climate warming, *Nat Geo*, 9, 584-589, 10.1038/ngeo2761, 2016.
- 1078 Gobiet, A., Kotlarski, S., Beniston, M., Heinrich, G., Rajczak, J., and Stoffel, M.: 21st century climate change in
1079 the European Alps - A review, *Science of the Total Environment*, 493, 1138-1151,
1080 10.1016/j.scitotenv.2013.07.050, 2014.
- 1081 [Grünewald, T., and Lehning, M.: Are flat-field snow depth measurements representative? A comparison of](#)
1082 [selected index sites with areal snow depth measurements at the small catchment scale, *Hydrol Processes*, 29,](#)
1083 [1717-1728, 10.1002/hyp.10295, 2015.](#)

- 1084 Hantel, M., Maurer, C., and Mayer, D.: The snowline climate of the Alps 1961–2010. *Theor Appl Climatol*, 110,
1085 517, 10.1007/s00704-012-0688-9, 2012.
- 1086 Hawkins, E., and Sutton, R.: The Potential to Narrow Uncertainty in Regional Climate Predictions, *B Am Meteorol*
1087 *Soc*, 90, 1095–+, 10.1175/2009BAMS2607.1, 2009.
- 1088 Haylock, M.R., Hofstra, N., Klein Tank, A.M.G., Klok, E.J., Jones, P.D., and New, M.: A European daily high-
1089 resolution gridded data set of surface temperature and precipitation for 1950–2006, *J Geophys Res*, 113,
1090 D20119, 10.1029/2008JD010201.
- 1091 Held, I. M., and Soden, B. J.: Robust responses of the hydrological cycle to global warming, *J Climate*, 19, 5686-
1092 5699, 10.1175/Jcli3990.1, 2006.
- 1093 IPCC: Climate Change 2013: The Physical Science Basis. Contribution of Working Group I to the Fifth
1094 Assessment Report of the Intergovernmental Panel on Climate Change, Cambridge University Press, Cambridge,
1095 United Kingdom and New York, NY, USA, 1535 pp., 2013.
- 1096 Isotta, F. A., Frei, C., Weilguni, V., Tadic, M. P., Lassegues, P., Rudolf, B., Pavan, V., Cacciamani, C., Antolini,
1097 G., Ratto, S. M., Munari, M., Micheletti, S., Bonati, V., Lussana, C., Ronchi, C., Panettieri, E., Marigo, G., and
1098 Vertacnik, G.: The climate of daily precipitation in the Alps: development and analysis of a high-resolution grid
1099 dataset from pan-Alpine rain-gauge data, *Int J Climatol*, 34, 1657-1675, 10.1002/joc.3794, 2014.
- 1100 Jacob, D., Petersen, J., Eggert, B., Alias, A., Christensen, O. B., Bouwer, L. M., Braun, A., Colette, A., Déqué, M.,
1101 Georgievski, G., Georgopoulou, E., Gobiet, A., Menut, L., Nikulin, G., Haensler, A., Hempelmann, N., Jones, C.,
1102 Keuler, K., Kovats, S., Kröner, N., Kotlarski, S., Kriegsman, A., Martin, E., van Meijgaard, E., Moseley, C.,
1103 Pfeifer, S., Preuschmann, S., Radermacher, C., Radtke, K., Rechid, D., Rounsevell, M., Samuelsson, P., Somot,
1104 S., Soussana, J. F., Teichmann, C., Valentini, R., Vautard, R., Weber, B., and Yiou, P.: EURO-CORDEX: new
1105 high-resolution climate change projections for European impact research, *Reg Environ Change*, 14, 563-578,
1106 10.1007/s10113-013-0499-2, 2014.
- 1107 Keller, D. E., Fischer, A. M., Liniger, M. A., Appenzeller, C. and Knutti, R.: Testing a weather generator for
1108 downscaling climate change projections over Switzerland. *Int J Climatol*, doi:10.1002/joc.4750, 2016.
- 1109 Kienzle, S. W.: A new temperature based method to separate rain and snow, *Hydrol Process*, 22, 5067-5085,
1110 10.1002/hyp.7131, 2008.
- 1111 [Kotlarski, S., Bosshard, T., Lüthi, D., Pall, P., and Schär, C.: Elevation gradients of European climate change in
1112 the regional climate model COSMO-CLM. *Clim Change*, 112, 189-215, 10.1007/s10584-011-0195-5, 2012.](#)
- 1113 Kotlarski, S., Keuler, K., Christensen, O. B., Colette, A., Deque, M., Gobiet, A., Goergen, K., Jacob, D., Luthi, D.,
1114 van Meijgaard, E., Nikulin, G., Schar, C., Teichmann, C., Vautard, R., Warrach-Sagi, K., and Wulfmeyer, V.:
1115 Regional climate modeling on European scales: a joint standard evaluation of the EURO-CORDEX RCM
1116 ensemble, *Geosci Model Dev*, 7, 1297-1333, 10.5194/gmd-7-1297-2014, 2014.
- 1117 Kotlarski, S., Lüthi, D., and Schär, C.: The elevation dependency of 21st century European climate change: an
1118 RCM ensemble perspective, *Int J Climatol*, 35, 3902-3920, 10.1002/joc.4254, 2015.
- 1119 Krasting, J. P., Broccoli, A. J., Dixon, K. W., and Lanzante, J. R.: Future Changes in Northern Hemisphere
1120 Snowfall. *J Clim*, 26, 7813-7828, 10.1175/JCLI-D-12-00832.1, 2013.
- 1121 Laternser, M., and Schneebeli, M.: Long-term snow climate trends of the Swiss Alps (1931-99), *Int J Climatol*, 23,
1122 733-750, 10.1002/joc.912, 2003.
- 1123 Marty, C.: Regime shift of snow days in Switzerland, *Geophys Res Lett*, 35, 10.1029/2008gl033998, 2008.
- 1124 Marty, C., and Blanchet, J.: Long-term changes in annual maximum snow depth and snowfall in Switzerland
1125 based on extreme value statistics, *Climatic Change*, 111, 705-721, 2011.
- 1126 McAfee, S. A., Walsh, J., and Rupp, T. S.: Statistically downscaled projections of snow/rain partitioning for
1127 Alaska, *Hydrol Process*, 28, 3930-3946, 10.1002/hyp.9934, 2014.
- 1128 [MeteoSchweiz: Klimareport 2015. Bundesamt für Meteorologie und Klimatologie MeteoSchweiz, Zürich.](#)
- 1129 MeteoSwiss: Daily Precipitation (final analysis): RhiresD:
1130 [www.meteoswiss.admin.ch/content/dam/meteoswiss/de/service-und-publikationen/produkt/raeumliche-daten-](http://www.meteoswiss.admin.ch/content/dam/meteoswiss/de/service-und-publikationen/produkt/raeumliche-daten-niederschlag/doc/ProdDoc_RhiresD.pdf)
1131 [niederschlag/doc/ProdDoc_RhiresD.pdf](http://www.meteoswiss.admin.ch/content/dam/meteoswiss/de/service-und-publikationen/produkt/raeumliche-daten-niederschlag/doc/ProdDoc_RhiresD.pdf), access: 10.01.2017, 2013a.
- 1132 MeteoSwiss: Daily Mean, Minimum and Maximum Temperature: TabsD, TminD, TmaxD:
1133 [www.meteoswiss.admin.ch/content/dam/meteoswiss/de/service-und-publikationen/produkt/raeumliche-daten-](http://www.meteoswiss.admin.ch/content/dam/meteoswiss/de/service-und-publikationen/produkt/raeumliche-daten-temperatur/doc/ProdDoc_TabsD.pdf)
1134 [temperatur/doc/ProdDoc_TabsD.pdf](http://www.meteoswiss.admin.ch/content/dam/meteoswiss/de/service-und-publikationen/produkt/raeumliche-daten-temperatur/doc/ProdDoc_TabsD.pdf), access: 10.01.2017, 2013b.
- 1135 Moss, R. H., Edmonds, J. A., Hibbard, K. A., Manning, M. R., Rose, S. K., van Vuuren, D. P., Carter, T. R., Emori,
1136 S., Kainuma, M., Kram, T., Meehl, G. A., Mitchell, J. F. B., Nakicenovic, N., Riahi, K., Smith, S. J., Stouffer, R. J.,
1137 Thomson, A. M., Weyant, J. P., and Wilbanks, T. J.: The next generation of scenarios for climate change research
1138 and assessment, *Nature*, 463, 747-756, 10.1038/nature08823, 2010.

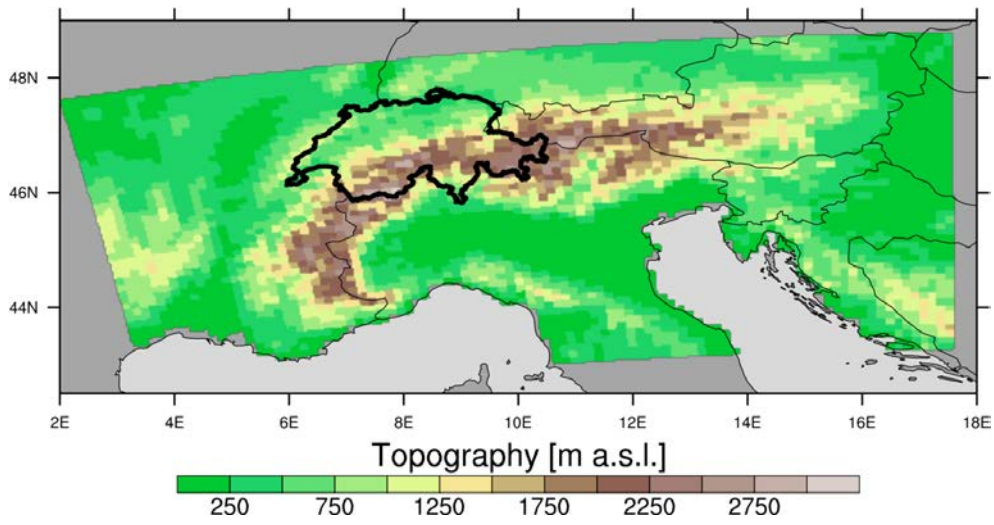
- 1139 Neff, E. L.: How Much Rain Does a Rain Gauge Gauge, *J Hydrol*, 35, 213-220, 10.1016/0022-1694(77)90001-4,
1140 1977.
- 1141 O'Gorman, P. A.: Contrasting responses of mean and extreme snowfall to climate change, *Nature*, 512, 416-
1142 U401, 10.1038/nature13625, 2014.
- 1143 Piazza, M., Boé, J., Terray, L., Pagé, C., Sanchez-Gomez, E., and Déqué, M.: Projected 21st century snowfall
1144 changes over the French Alps and related uncertainties, *Climatic Change*, 122, 583-594, 10.1007/s10584-013-
1145 1017-8, 2014.
- 1146 Räisänen, J.: Twenty-first century changes in snowfall climate in Northern Europe in ENSEMBLES regional
1147 climate models, *Clim Dynam*, 46, 339-353, 10.1007/s00382-015-2587-0, 2016.
- 1148 Rajczak, J., Pall, P., and Schär, C.: Projections of extreme precipitation events in regional climate simulations for
1149 Europe and the Alpine Region, *J Geophys Res-Atmos*, 118, 3610-3626, 10.1002/jgrd.50297, 2013.
- 1150 Rajczak, J., Kotlarski, S., and Schär, C.: Does Quantile Mapping of Simulated Precipitation Correct for Biases in
1151 Transition Probabilities and Spell Lengths?, *J Climate*, 29, 1605-1615, 10.1175/Jcli-D-15-0162.1, 2016.
- 1152 Rajczak, J. and Schär, C.: Projections of future precipitation extremes over Europe: A multi-model assessment of
1153 climate simulations. In preparation.
- 1154 Richards, F. J.: A Flexible Growth Function for Empirical Use, *J Exp Bot*, 10, 290-300, 10.1093/Jxb/10.2.290,
1155 1959.
- 1156 Rummukainen, M.: State-of-the-art with regional climate models, *Wiley Interdisciplinary Reviews-Climate Change*,
1157 1, 82-96, 10.1002/wcc.8, 2010.
- 1158 Schär, C., Ban, N., Fischer, E. M., Rajczak, J., Schmidli, J., Frei, C., Giorgi, F., Karl, T. R., Kendon, E. J., Tank, A.
1159 M. G. K., O'Gorman, P. A., Sillmann, J., Zhang, X. B., and Zwiers, F. W.: Percentile indices for assessing changes
1160 in heavy precipitation events, *Climatic Change*, 137, 201-216, 10.1007/s10584-016-1669-2, 2016.
- 1161 Scherrer, S. C., Appenzeller, C., and Laternser, M.: Trends in Swiss Alpine snow days: The role of local- and
1162 large-scale climate variability, *Geophys Res Lett*, 31, 10.1029/2004gl020255, 2004.
- 1163 Schmidli, J., Frei, C., and Vidale, P. L.: Downscaling from GCM precipitation: A benchmark for dynamical and
1164 statistical downscaling methods, *Int J Climatol*, 26, 679-689, 10.1002/joc.1287, 2006.
- 1165 Schmucki, E., Marty, C., Fierz, C., and Lehning, M.: Simulations of 21st century snow response to climate change
1166 in Switzerland from a set of RCMs, *Int J Climatol*, 35, 3262-3273, 10.1002/joc.4205, 2015a.
- 1167 Schmucki, E., Marty, C., Fierz, C., Weingartner, R. and Lehning, M.: Impact of climate change in Switzerland on
1168 socioeconomic snow indices, *Theor Appl Climatol*, in press, 10.1007/s00704-015-1676-7, 2015b.
- 1169 Serquet, G., Marty, C., and Rebetez, M.: Monthly trends and the corresponding altitudinal shift in the
1170 snowfall/precipitation day ratio, *Theor Appl Climatol*, 114, 437-444, 10.1007/s00704-013-0847-7, 2013.
- 1171 Der Niederschlag in der Schweiz, Geographisches Institut der Eidgenössischen Technischen Hochschule in
1172 Zürich, Abteilung Hydrologie, Zurich, Switzerland, 1985.
- 1173 SFOE, Hydropower: <http://www.bfe.admin.ch/themen/00490/00491/index.html?lang=en>, access: 16.09.2016,
1174 2014.
- 1175 Smiatek, G., Kunstmann, H., and Senatore, A.: EURO-CORDEX regional climate model analysis for the Greater
1176 Alpine Region: Performance and expected future change, *J Geophys Res-Atmos*, 121, 7710-7728,
1177 10.1002/2015JD024727, 2016.
- 1178 Soncini, A., and Bocchiola, D.: Assessment of future snowfall regimes within the Italian Alps using general
1179 circulation models, *Cold Reg Sci Technol*, 68, 113-123, 10.1016/j.coldregions.2011.06.011, 2011.
- 1180 Steger, C., Kotlarski, S., Jonas, T., and Schär, C.: Alpine snow cover in a changing climate: a regional climate
1181 model perspective, *Clim Dynam*, 41, 735-754, 10.1007/s00382-012-1545-3, 2013.
- 1182 Techel, F., Stucki, T., Margreth, S., Marty, C., and Winkler, K.: Schnee und Lawinen in den Schweizer Alpen.
1183 Hydrologisches Jahr 2013/14, WSL-Institut für Schnee- und Lawinenforschung SLF, Birmensdorf, Switzerland,
1184 2015.
- 1185 Terzago, S., von Hardenberg, J., Palazzi, E., and Provenzale, A.: Snow water equivalent in the Alps as seen by
1186 gridded datasets, CMIP5 and CORDEX climate models. *The Cryosphere Discussion*, 10.5194/tc-2016-280, 2017.
- 1187 Torma, C., Giorgi, F., and Coppola, E.: Added value of regional climate modeling over areas characterized by
1188 complex terrain Precipitation over the Alps, *J Geophys Res-Atmos*, 120, 3957-3972, 10.1002/2014JD022781,
1189 2015.
- 1190 Vautard, R., Gobiet, A., Jacob, D., Belda, M., Colette, A., Déqué, M., Fernandez, J., Garcia-Diez, M., Goergen,
1191 K., Guttler, I., Halenka, T., Karacostas, T., Katragkou, E., Keuler, K., Kotlarski, S., Mayer, S., van Meijgaard, E.,
1192 Nikulin, G., Patarcic, M., Scinocca, J., Sobolowski, S., Suklitsch, M., Teichmann, C., Warrach-Sagi, K.,
1193 Wulfmeyer, V., and Yiou, P.: The simulation of European heat waves from an ensemble of regional climate
1194 models within the EURO-CORDEX project, *Clim Dynam*, 41, 2555-2575, 10.1007/s00382-013-1714-z, 2013.

- 1195 Weingartner, R., Schädler, B., and Hänggi, P.: Auswirkungen der Klimaänderung auf die schweizerische
1196 Wasserkraftnutzung, *Geographica Helvetica*, 68, 239-248, 2013.
- 1197 Yang, D. Q., Elomaa, E., Tuominen, A., Aaltonen, A., Goodison, B., Gunther, T., Golubev, V., Sevruk, B.,
1198 Madsen, H., and Milkovic, J.: Wind-induced precipitation undercatch of the Hellmann gauges, *Nord Hydrol*, 30,
1199 57-80, 1999.
- 1200 Zubler, E. M., Scherrer, S. C., Croci-Maspoli, M., Liniger, M. A., and Appenzeller, C.: Key climate indices in
1201 Switzerland; expected changes in a future climate, *Climatic Change*, 123, 255-271, 10.1007/s10584-013-1041-8,
1202 2014.
- 1203 Zubler, E. M., Fischer, A. M., Liniger, M. A., and Schlegel, T.: Auftausalzverbrauch im Klimawandel, MeteoSwiss,
1204 Zurich, Switzerland, Fachbericht 253, 2015.
- 1205

1206 **Figures**

1207

1208

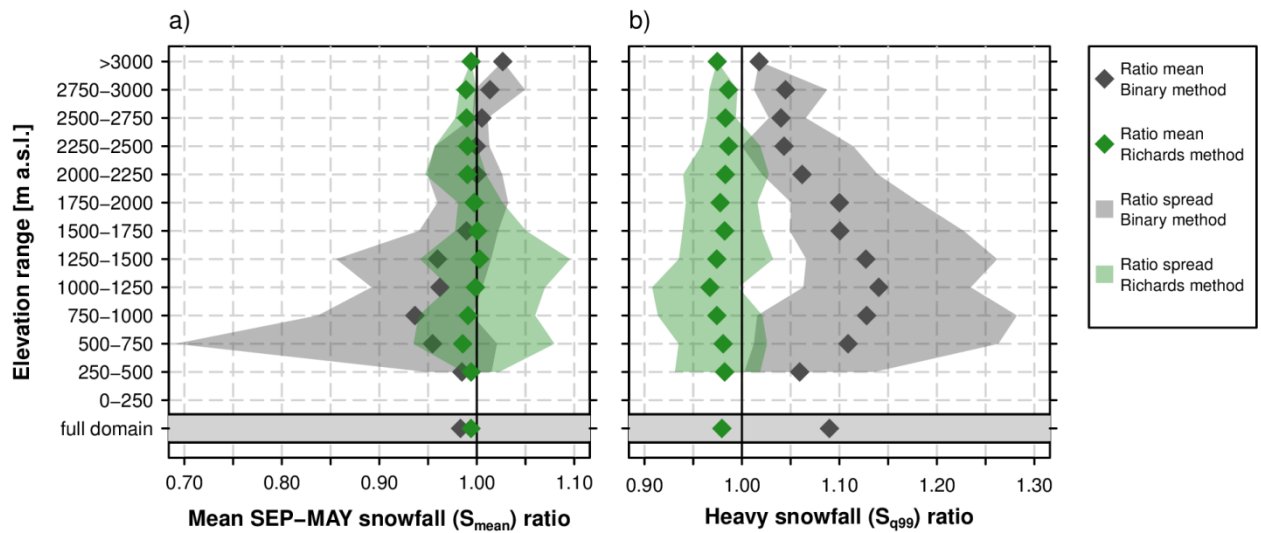


1209

1210

1211 **Figure 1** GTOPO30 ~~t~~Topography (<https://ita.cr.usgs.gov/GTOPO30>) aggregated to the ~~at~~EUR-11 (0.11°) RCM
1212 grid. resolution of ~~The coloured area shows~~ the Alpine domain used for the assessment of snowfall projections.
1213 The bold black outline marks the Swiss sub-domain used for the assessment of the bias adjustment~~correction~~
1214 approach.

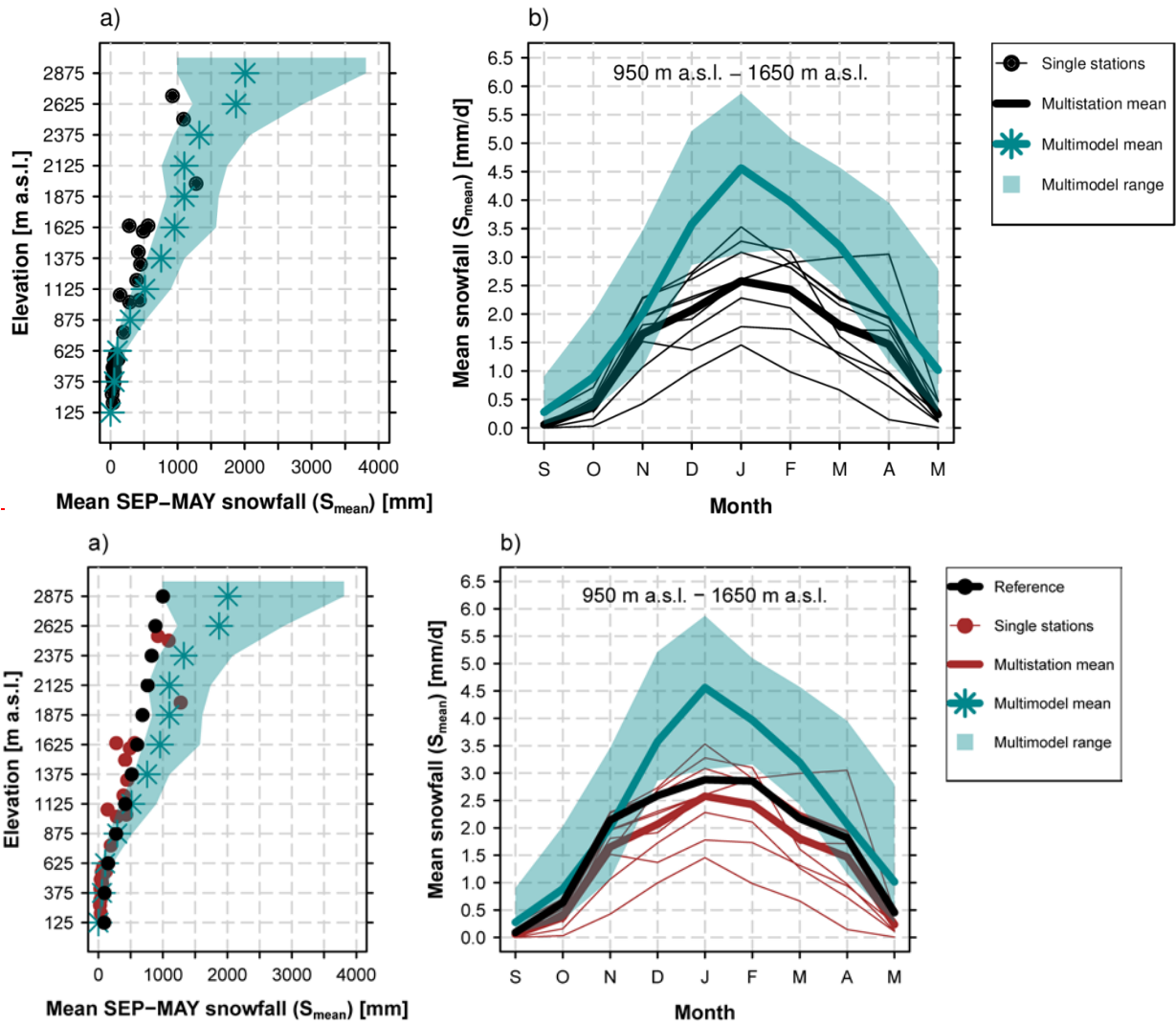
1215



1216
1217

1218 **Figure 2** Snowfall ratios for the Binary and Richards snow fractionation method (ratio between the snowfall of the
 1219 respective method and the ~~full-subgrid-snow-representation~~ Subgrid method). The ratios are valid at the coarse-
 1220 resolution grid (12 km). a) Ratios for mean snowfall, S_{mean} . b) Ratios for heavy snowfall, S_{q99} . Ratio means were
 1221 derived after averaging the corresponding snowfall index for 250 m elevation intervals in Switzerland while the
 1222 ratio spread represents the minimum and maximum grid point-based ratios in the corresponding elevation
 1223 interval. This analysis is entirely based on the observational data sets TabsD and RhiresD.

1224

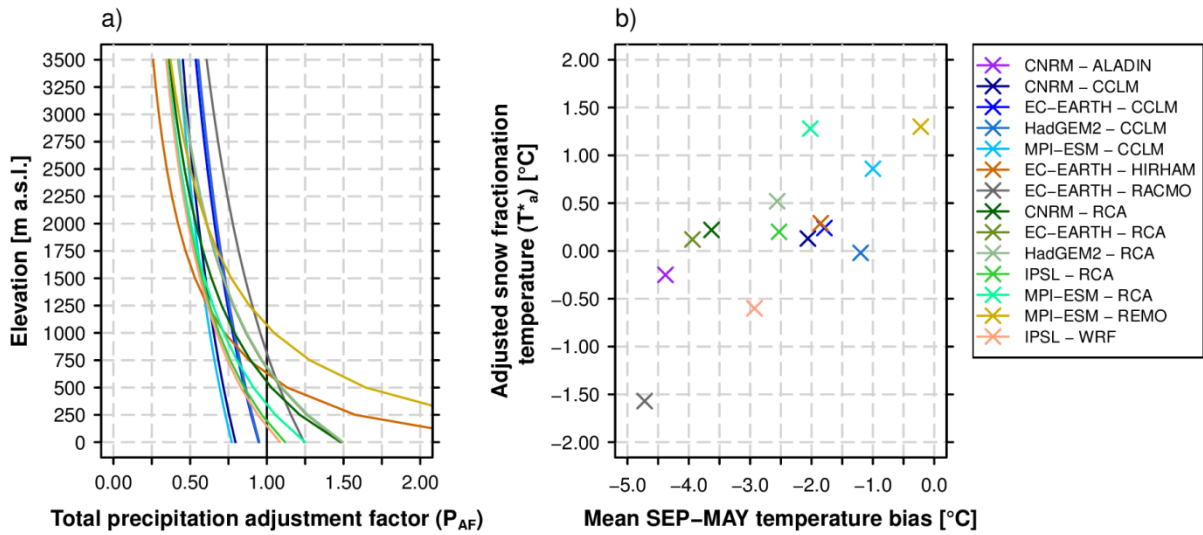


1225

1226

1227 **Figure 3** Comparison of measured fresh snow sums of 29 MeteoSwiss stations (red) against vs. simulated RCM
 1228 raw snowfall in Switzerland (green) and against the 2 km reference snowfall grid obtained by employing the
 1229 *Subgrid method* (black) in the EVAL period 1971-2005. a) Mean September – May snowfall vs. elevation. Both
 1230 the simulation data (green) and the reference data (black) are based on the spatio-temporal mean of 250 m
 1231 elevation ranges and plotted at the mean elevation of the corresponding interval. b) Seasonal September-May
 1232 snowfall cycle for the elevation interval 950 m a.s.l. to 1650 m a.s.l.. Simulated multi-model means and spreads
 1233 are based on a subset of 9 EURO-CORDEX simulations providing raw snowfall as output variable (see Tab. 1).

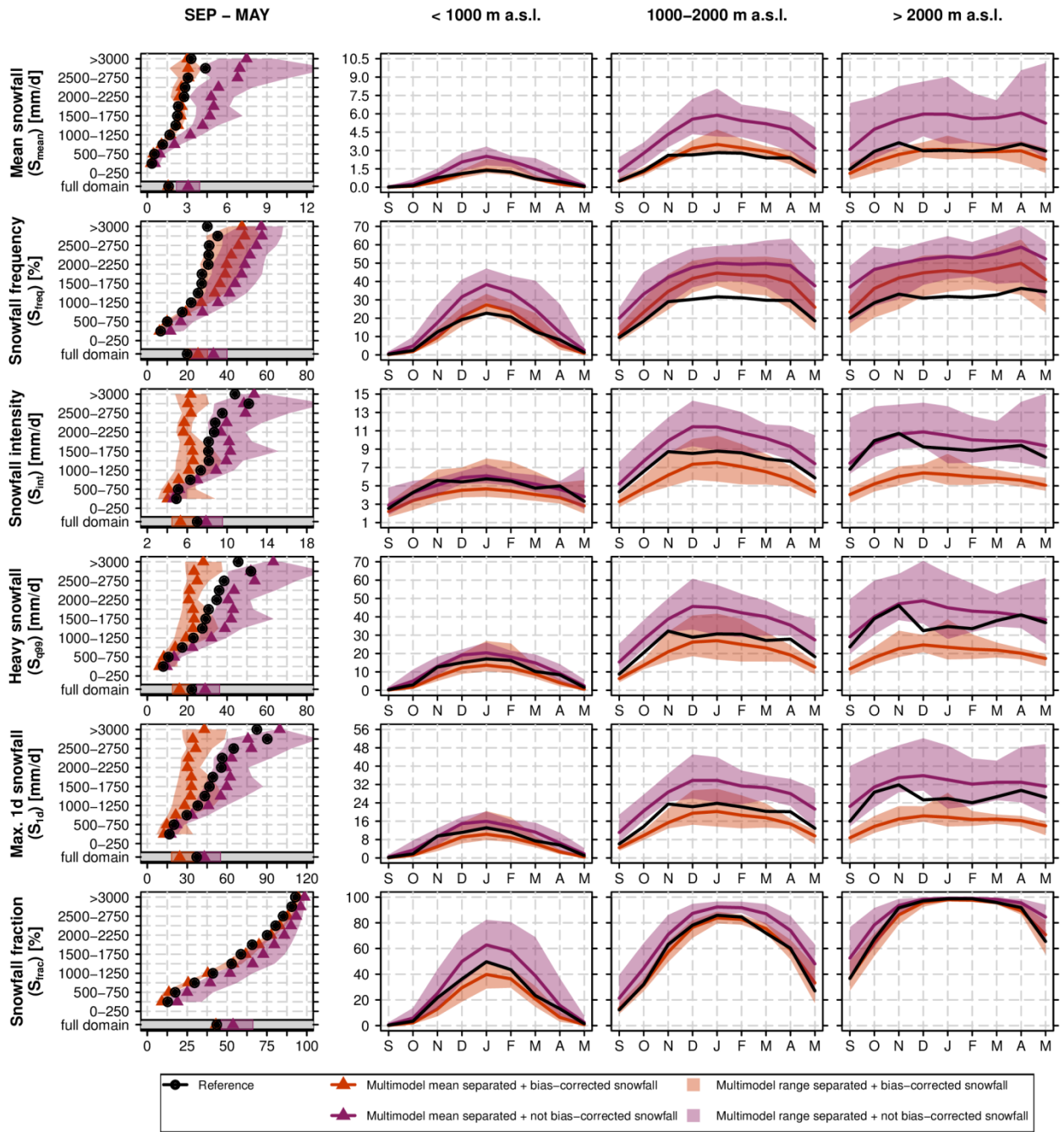
1234



1235

1236

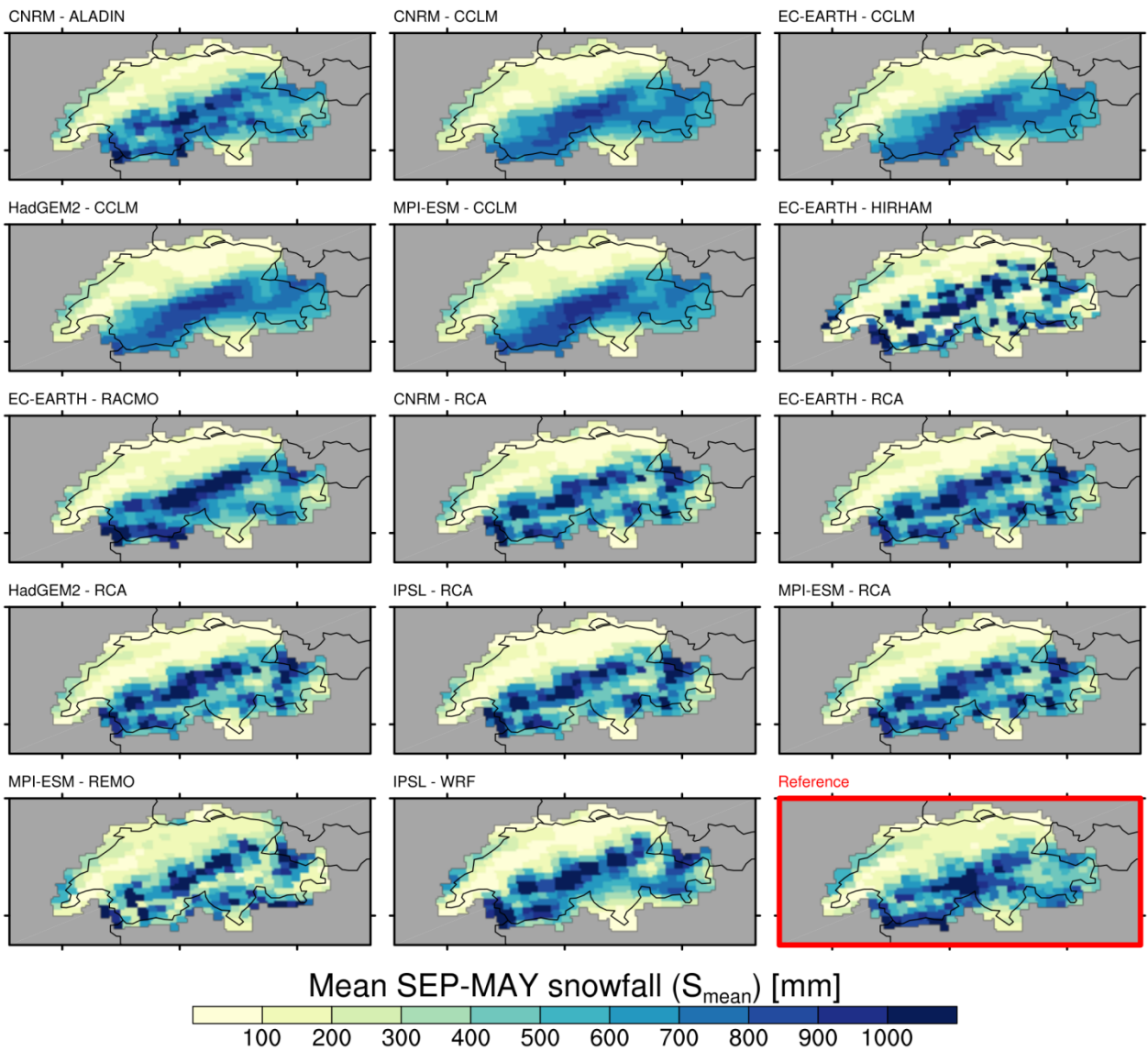
1237 | **Figure 4** ~~Bias correction and adjustment factors~~ Overview on bias adjustment. a) Elevation-dependent total
 1238 precipitation adjustment factors, P_{AF} , for the 14 GCM-RCM chains (see Eq. 10). b) Scatterplot of mean September
 1239 to May temperature biases (RCM simulation minus observational analysis) vs. adjusted snow fractionation
 1240 temperatures, T^*_a .



1241
1242

1243 **Figure 5** Evaluation of snowfall indices in the EVAL period 1971-2005 for the 14 snowfall separated + bias-
 1244 corrected-adjusted ($RCM_{sep+bae}$) and 14 snowfall separated + not bias-corrected-adjusted ($RCM_{sep+nb_{ae}}$) RCM
 1245 simulations vs. observation-based reference. The first column shows the mean September-May snowfall index
 1246 statistics vs. elevation while the monthly snowfall indices (spatially averaged over the elevation intervals <1000
 1247 m a.s.l., 1000 m a.s.l.-2000 m a.s.l. and >2000 m a.s.l.) are displayed in columns 2-4.

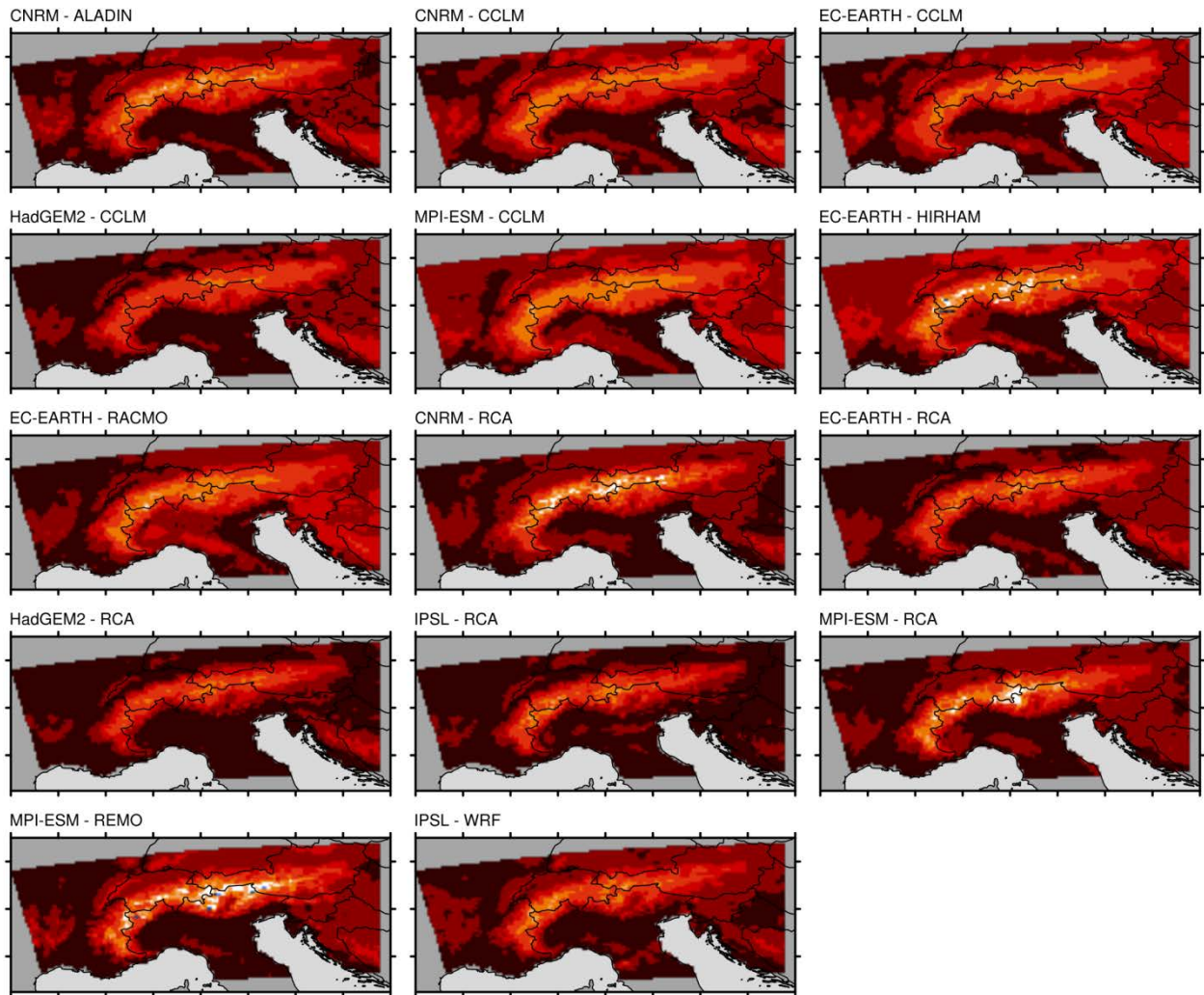
1248



1249
1250

1251 **Figure 6** Spatial distribution of mean September-May snowfall, S_{mean} , in the EVAL period 1971-2005 and for the
 1252 | 14 snowfall separated + bias-~~corrected~~-adjusted RCM simulations ($\text{RCM}_{\text{sep}+\text{bae}}$). In the lower right panel, the map
 1253 of the observation-based reference is shown.

1254



Mean SEP-MAY snowfall change (δS_{mean}) [%], RCP8.5



1255

1256

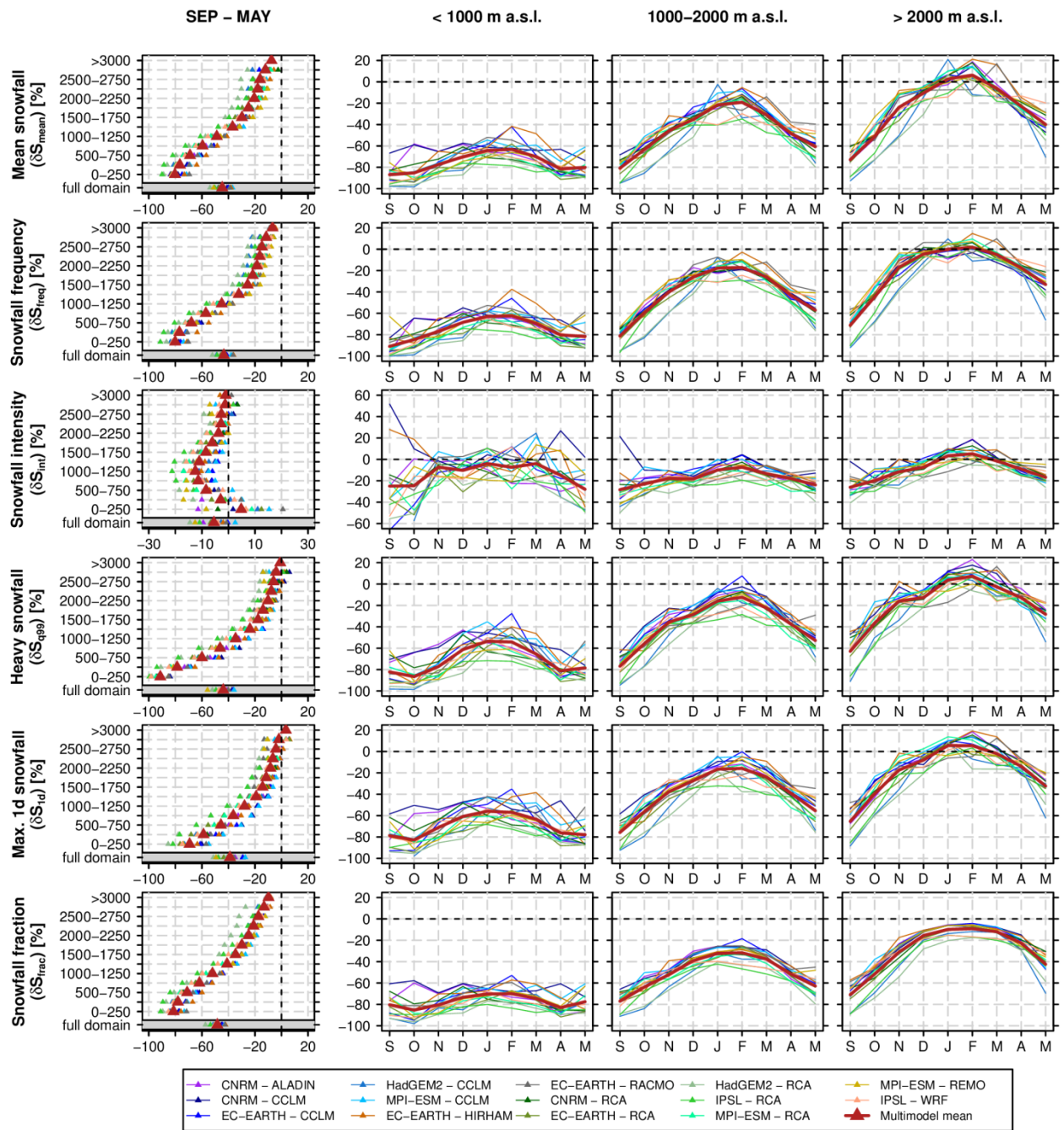
1257

1258

1259

1260

Figure 7 Spatial distribution of relative changes (SCEN period 2070-2099 with respect to CTRL period 1981-2010) in mean September-May snowfall, δS_{mean} , for RCP8.5 and for the 14 snowfall separated + bias_~~corrected~~ adjusted RCM simulations ($\text{RCM}_{\text{sep+b3e}}$). For RCP4.5, see Fig. S65.



1261

1262

1263

1264

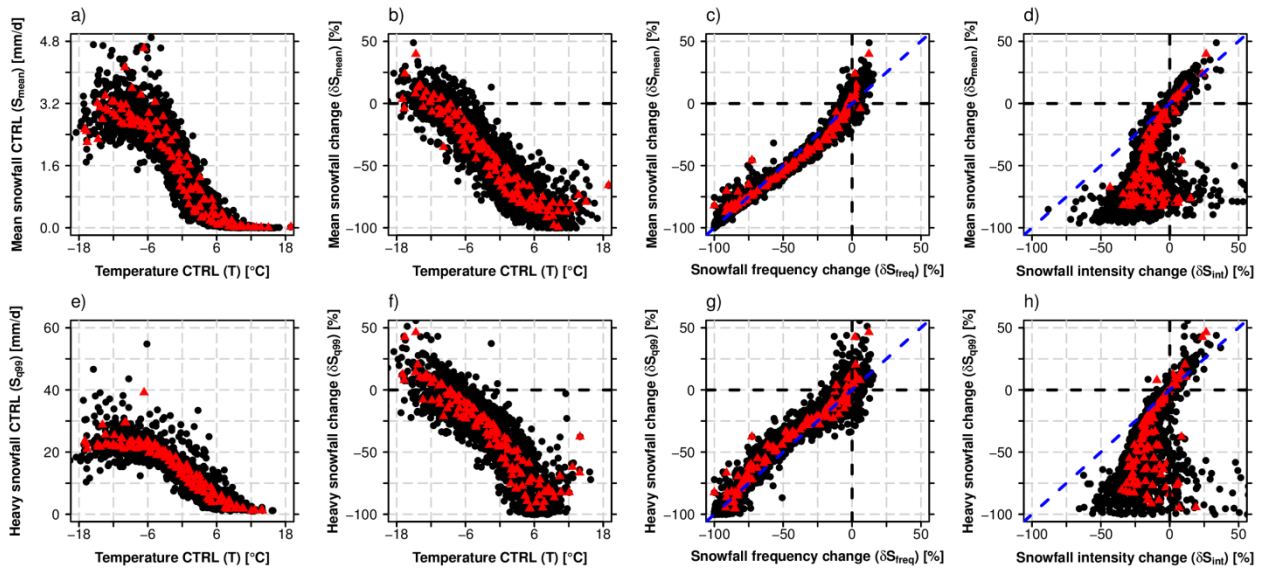
1265

1266

1267

1268

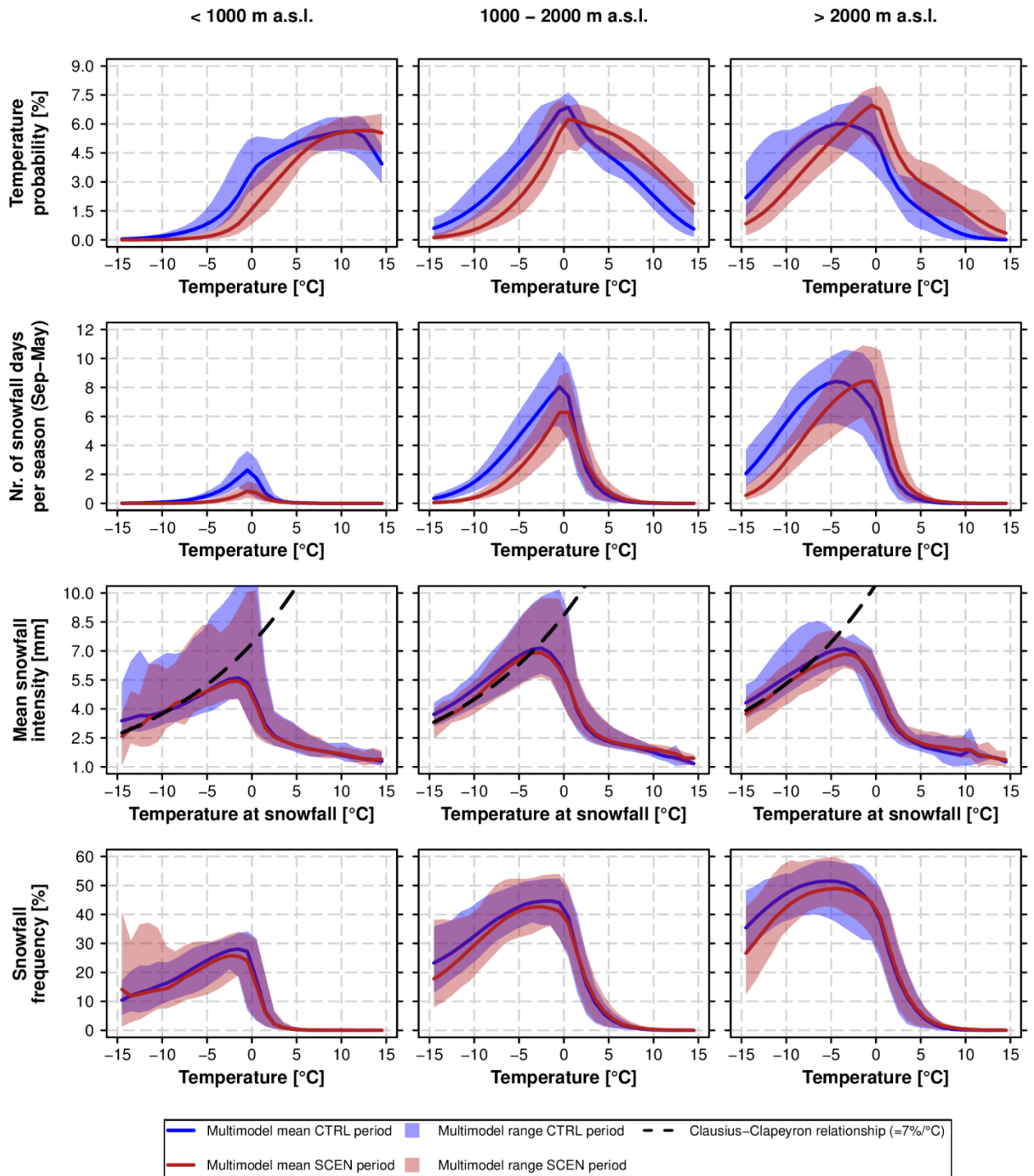
Figure 8 Relative changes (SCEN period 2070-2099 with respect to CTRL period 1981-2010) of snowfall indices based on the 14 snowfall separated + bias-corrected-adjusted RCM simulations (RCM_{sep+bc}) for RCP8.5. The first column shows the mean September-May snowfall index statistics vs. elevation while monthly snowfall index changes (spatially averaged over the elevation intervals <1000 m.a.s.l., 1000 m a.s.l.-2000 m a.s.l. and >2000 m a.s.l.) are displayed in columns 2-4.



1269
1270

1271 **Figure 9** Intercomparison of various snowfall indices and relationship with monthly mean temperature in CTRL.
 1272 For each panel, the monthly mean statistics for each 250 m elevation interval and for each of the 14 individual
 1273 GCM-RCM chains were derived (black circles). Red triangles denote the multi-model mean for a specific month
 1274 and elevation interval. The monthly statistics were calculated by considering all grid points of the specific
 1275 elevation intervals which are available for both variables in the corresponding scatterplot only (area consistency).
 1276 The data were taken from the 14 snowfall separated + bias-corrected-adjusted (RCM_{sep+bias}) RCM simulations.
 1277 Relative changes are based on the RCP8.5 driven simulations (SCEN 2070-2099 wrt. CTRL 1981-2010).

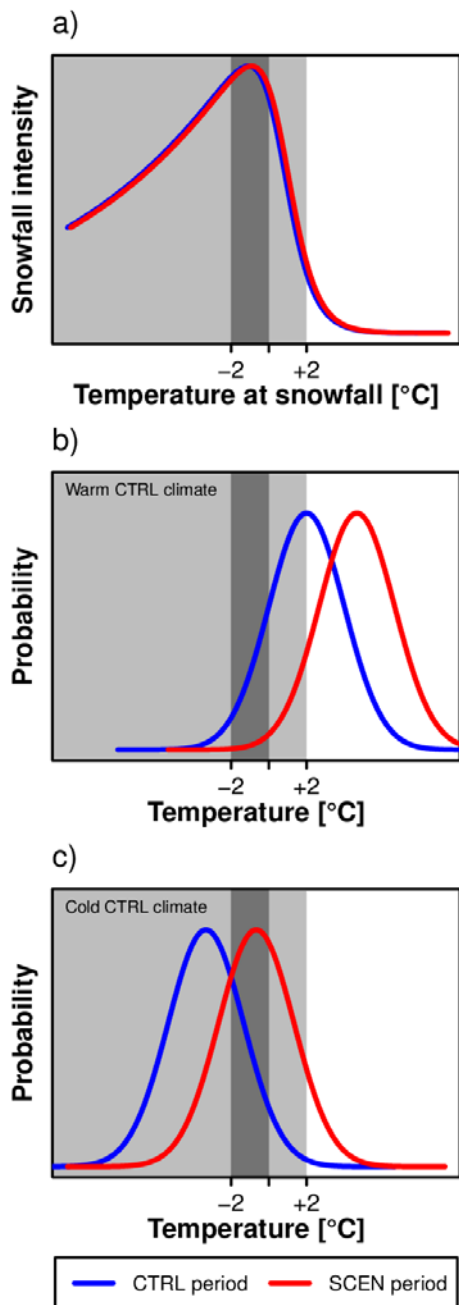
1278



1279

1280

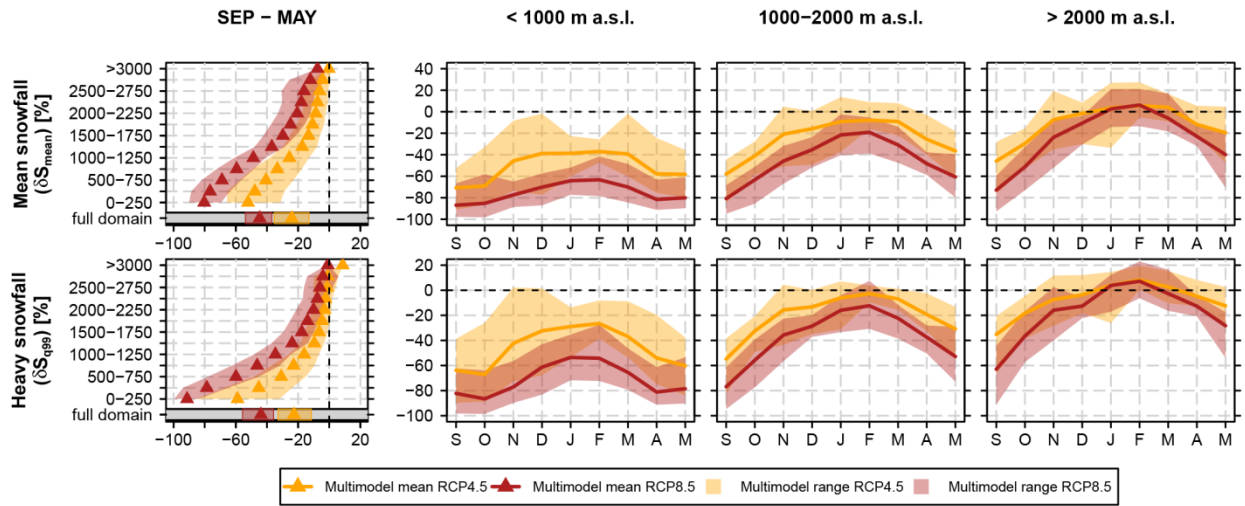
1281 **Figure 10** Comparison of temperature probability, snowfall probability and mean snowfall intensity for the CTRL
1282 period 1981-2010 and SCEN period 2070-2099 for RCP8.5. The analysis is based on data from the 14 snowfall
1283 separated + bias_~~corrected~~_adjusted RCM simulations (RCM_{sep+bae}). The top row depicts the PDF of the daily
1284 temperature distribution, while the second row shows the mean number of snowfall days between September and
1285 May, i.e., days with $S > 1 \text{ mm/d}$ (see Tab. 2), in a particular temperature interval. The third row represents the
1286 mean snowfall intensity, S_{int} , for a given snowfall temperature interval. In addition the Clausius-Clapeyron
1287 relationship, centred at the -10°C mean S_{int} for SCEN, is displayed by the black dashed line. PDFs and mean S_{int}
1288 were calculated by creating daily mean temperature bins of width 1°C .



1289
1290

1291 **Figure 11** Schematic illustration of the control of changes in snowfall intensity on changes in mean and extreme
 1292 snowfall. a) Relation between temperature and mean snowfall intensity. b) Daily temperature PDF for a warm
 1293 control climate (low elevations or transition seasons, i.e., beginning or end of winter). c) Daily temperature PDF
 1294 for a cold control climate (high elevations or mid-winter). The blue line denotes the historical CTRL period, the red
 1295 line the future SCEN period. The light grey shaded area represents the overall temperature interval at which
 1296 snowfall occurs, the dark grey shading shows the preferred temperature interval for heavy snowfall to occur.

1297



1298

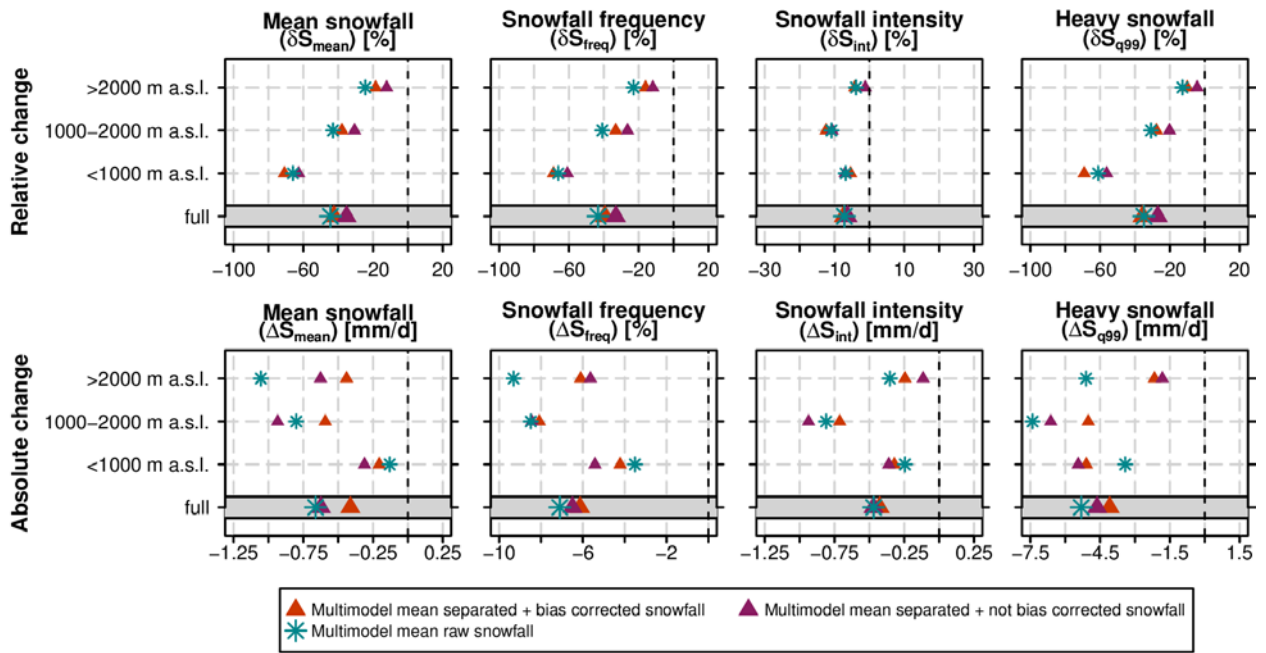
1299

1300

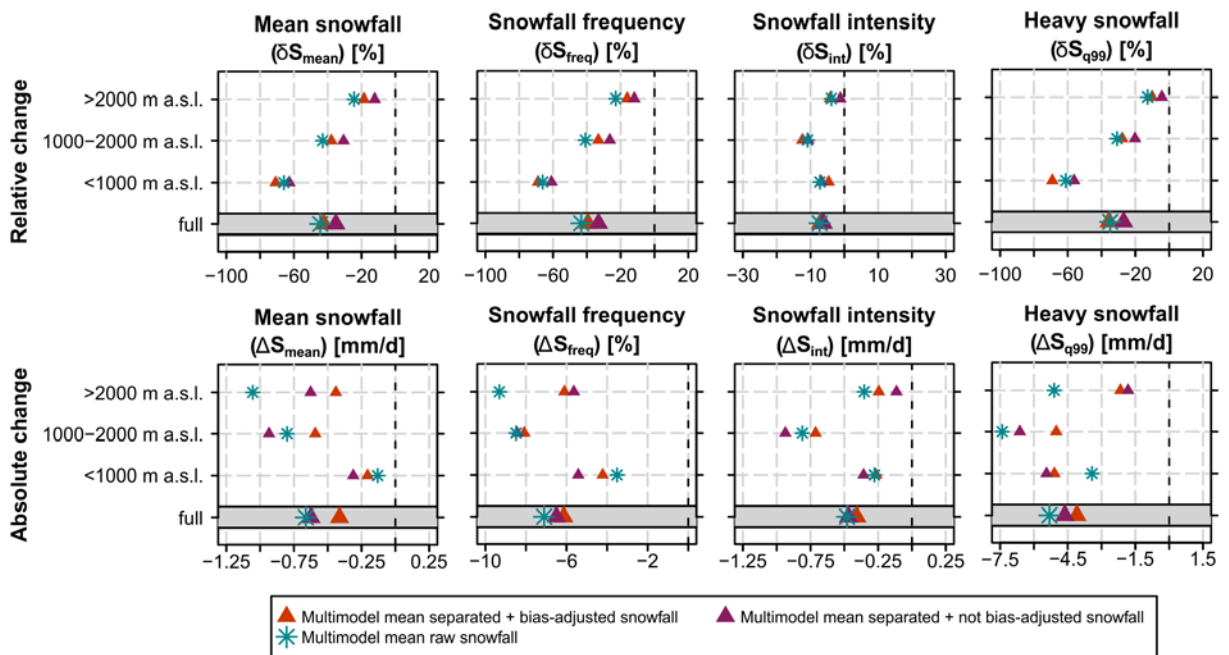
1301

Figure 12 Similar as Figure 8 but showing projected changes of mean snowfall, δS_{mean} , and heavy snowfall, δS_{q99} , for the emission scenarios RCP4.5 and 8.5. See Fig. S98 for the emission scenario uncertainty of the remaining four snowfall indices.

1302



1303
1304



1305
1306
1307
1308
1309
1310

Figure 13 Relative and absolute changes (SCEN period 2070-2099 with respect to CTRL period 1981-2010) of mean September-May snowfall indices based on a subset of 9 snowfall separated + bias-~~corrected~~-adjusted (RCM_{sep+bae}), 9 snowfall separated + not bias-~~corrected~~-adjusted (RCM_{sep+nbae}) and 9 raw snowfall RCM simulations (RCM_{raw}) for RCP8.5. Only RCM simulations providing raw snowfall as output variable (see Tab. 1) were used in this analysis.

1311

1312 **Tables**

1313

1314 | **Table 1** Overview on the 14 EURO-CORDEX simulations available for this study. The whole model set consists of
 1315 | seven RCMs driven by five different GCMs. All experiments were realized on a grid, covering the European
 1316 | domain, with a horizontal resolution of approximately 12.5 km (EUR-11) and were run for control RCP4.5 and
 1317 | RCP8.5 scenarios within the considered time periods of interest. A subset of 9 simulations provides raw snowfall,
 1318 | i.e., snowfall flux in kg/m²s, as output variable. For full institutional names the reader is referred to the official
 1319 | EURO-CORDEX website www.euro-cordex.net. Note that the EC-EARTH-driven experiments partly employ
 1320 | different realizations of the GCM run, i.e., explicitly sample the influence of internal climate variability in addition to
 1321 | model uncertainty.

RCM	GCM	Acronym	Institute ID	Raw snowfall output
ALADIN53	CNRM-CERFACS-CNRM-CM5	CNRM - ALADIN	CNRM	no
CCLM4-8-17	CNRM-CERFACS-CNRM-CM5	CNRM - CCLM	CLMcom/BTU	no
CCLM4-8-17	ICHEC-EC-EARTH	EC-EARTH - CCLM	CLMcom/BTU	no
CCLM4-8-17	MOHC-HadGEM2-ES	HadGEM2 - CCLM	CLMcom/ETH	no
CCLM4-8-17	MPI-M-MPI-ESM-LR	MPI-ESM - CCLM	CLMcom/BTU	no
HIRHAM5	ICHEC-EC-EARTH	EC-EARTH - HIRHAM	DMI	yes
RACMO22E	ICHEC-EC-EARTH	EC-EARTH - RACMO	KNMI	yes
RCA4	CNRM-CERFACS-CNRM-CM5	CNRM - RCA	SMHI	yes
RCA4	ICHEC-EC-EARTH	EC-EARTH - RCA	SMHI	yes
-RCA4	MOHC-HadGEM2-ES	HadGEM2 - RCA	SMHI	yes
RCA4	IPSL-IPSL-CM5A-MR	IPSL - RCA	SMHI	yes
RCA4	MPI-M-MPI-ESM-LR	MPI-ESM – RCA	SMHI	yes
REMO2009	MPI-M-MPI-ESM-LR	MPI-ESM – REMO*	MPI-CSC	yes
WRF331F	IPSL-IPSL-CM5A-MR	IPSL - WRF	IPSL-INERIS	yes

* r1i1p1 realisation

1322

1323

1324 **Table 2** Analysed snowfall indices. The last column indicates the threshold value in the CTRL period for
 1325 considering a grid cell in the climate changes analysis (grid cells with smaller values are skipped for the
 1326 respective analysis); first number: threshold for monthly analyses, second number: threshold for seasonal
 1327 analysis.

Index name	Acronym	Unit	Definition	Threshold for monthly / seasonal analysis
Mean snowfall	S_{mean}	mm	(Spatio-)temporal mean snowfall in mm snow water equivalent (only "mm" thereafter).	1 mm / 10 mm
Heavy snowfall	S_{q99}	mm/d	Grid point-based 99% all day snowfall percentile.	1 mm / 1 mm
Max. 1 day snowfall	S_{1d}	mm/d	Mean of each season's or month's maximum 1 day snowfall.	1 mm / 1 mm
Snowfall frequency	S_{freq}	%	Percentage of days with snowfall $S > 1$ mm/d within a specific time period.	1 % / 1 %
Snowfall intensity	S_{int}	mm/d	Mean snowfall intensity at days with snowfall $S > 1$ mm/d within a specific time period.	S_{freq} threshold passed
Snowfall fraction	S_{frac}	%	Percentage of total snowfall, S_{tot} , on total precipitation, P_{tot} , within a specific time period.	1 % / 1 %

1328
 1329
 1330
 1331